ROYAL SOCIETY OF CHEMISTRY

REVIEW

Check for updates

Conjugated polymer-based luminescent probes for ratiometric detection of biomolecules

Linfeng Zhao, Can Zhao, Jiasheng Zhou, Haiwei Ji, [ID] Yuling Qin, Guo Li,*
Li Wu [ID] * and Xiaobo Zhou*

Accurate monitoring of the biomolecular changes in biological and physiological environments is of great significance for the pathogenesis, development, diagnosis and treatment of diseases. Compared with traditional luminescent probes on the basis of an intensity-dependent single-channel readout, ratiometric fluorescence detection is a more reliable sensing or imaging method which can monitor different emission signals in two or more channels with a built-in self-calibration functionality, attracting growing attention in biomolecule detection. As a kind of luminescent material with many prospects, conjugated polymers with an easily functionalized organic molecular structure, high brightness, superior stability, tunable emission, and superior biocompatibility have been widely adopted as ratiometric fluorescent probes in biosensing and bioimaging. This review first summarizes the design principles of luminescent conjugated polymers that have been developed as methods for the ratiometric measurement of biomolecules. Additionally, their potential in accurate biodetection of living biosystems was investigated. This paper aims to provide a comprehensive review of the existing challenges and latest advancements in ratiometric detection of various biomolecules with high selectivity and sensitivity. We sincerely expect that the information presented in this review could inspire broader interests across various disciplines and stimulate more exciting achievements in biodetection for the benefit of biomedical research.

1. Introduction

Accurate monitoring of biomolecular expression levels in biological and physiological environments plays a key role in research on pathogenesis and therapies of diseases.[1–3] Various sensing and imaging techniques such as optical,[4]

School of Public Health, Nantong University, No. 9, Seyuan Road, Nantong 226019, China. E-mail: gli@ntu.edu.cn, wuli8686@ntu.edu.cn, xbzhou@ntu.edu.cn

radiographic,[5] magnetic[6] and electrochemical[7] techniques have been proposed and developed, realizing a wide application so far. Among the biosensing and bioimaging techniques that have been developed, fluorescence-based sensing and imaging techniques have attracted much attention due to their multiple advantageous features, including high sensitivity, good spatial and temporal resolution, real-time and *in situ* observability, non-invasiveness and low cost.[8–10] In the past few decades, numerous studies have verified the excellent analytical

Lingfeng Zhao is studying in the School of Public Health, Nantong University, under the direction of Dr Zhou Xiaobo and Prof. Wu Li. His research interests focus on the design and synthesis of luminescent nanoprobes and their bioapplications.

Linfeng Zhao

Dr Guo Li obtained his PhD degree under the direction of Professor Qiang Zhao from the Nanjing University of Posts & Telecommunications in 2020. He joined the School of Public Health, Nantong University, as an Associate Professor in 2020. His current research interests focus on the development of novel conjugated polymers for cancer theranostics.

Guo Li

performance and huge application potential of fluorescence sensing and imaging techniques in biomedical applications. However, most of the fluorescent probes previously reported indicate the variations of targets by monitoring the signal changes in a single fluorescence channel ("ON–OFF" or "OFF–ON" type). However, the single and intensity-based reporting signal which could easily be interfered by ambient environment factors, like temperature, pH or the concentration of ions, oxygen and lipid molecules, the concentration of probes and external excitation power, would bring about inaccurate sensing or imaging results. In contrast, the ratiometric fluorescence detection method with a built-in self-calibration function can provide more reliable sensing or imaging results by monitoring different emission signals in two or more channels simultaneously.[11–15] Benefiting from the above ratiometric design, accurate, real-time and dynamic tracking of biomolecule changes in complex environments, including in living cells or in living animals, can even be achieved.[16–21]

Considering their easily modified chemical structure and high fluorescence quantum yield, small-molecule organic dyes as fluorescent bioprobes have gained increasing popularity in the past few decades.[22,23] However, the inherent weaknesses of traditional small-molecule organic fluorescent dyes, such as poor photostability, low single-fluorophore brightness and fluorescence quenching at an aggregated state, limited their prospects in some biomedical applications where ultra-high sensitivity and long period real-time tracking are required.

Conjugated polymers (CPs) are excellent luminescent materials with delocalized electronic structures, which comprise numerous repeat units with conjugated chemical structures (Fig. 1). The unique chemical structure endows CPs with outstanding light-harvesting and signal amplification capacities, together with other properties including high fluorescence quantum yield, tunable emission wavelength and excellent photochemical stability (Table 1), thus displaying great potential in the construction of high-performance fluorescent biosensors.[24–26] Since most traditional CPs are of a large π-conjugated structure with strong hydrophobicity, it is difficult to apply them in biologically analytic scenarios directly. In order to give full play to the superior properties of CPs, mainly two methods for functionalizing the CPs in biological applications have been proposed so far. One is the so-called "conjugated polyelectrolyte (CPE)" strategy, which modifies the hydrophilic groups on the side chain of CPs in order to improve the hydrophilicity of CPs. The other method is to encapsulate the CPs into a water-dispersed nanocapsule that is assembled by the amphiphilic molecules, which is the so-called "semiconducting polymer nanoparticles (SNPs)" or "polymer dots (Pdots)". It is noteworthy that Pdots are defined as a kind of luminescent nanoparticle smaller than 20–30 nm in size and with a weight concentration or a volume fraction of hydrophobic CPs over 50% at least.[27–29] Therefore, in some studies, CPEs with poor water solubility are presented in the manner of self-assembled, small-sized nanoparticles (<20–30 nm) in aqueous solutions, and thus, they were also referred to as Pdots. The preparation of Pdots was mainly carried out using the methods of nanoprecipitation and mini-emulsion (Fig. 2). Owing to the exceptional photophysical properties of CPs, CP-derived fluorescent biosensors demonstrate desirable luminescence properties, including large extinction coefficient, tunable emission parameters (i.e., wavelength, lifetime, multiplicity of peak, and bandwidth), high brightness of single particle and superior photostability. As biosensing and bioimaging probes, their superior biocompatibility, modifiability and photo/chemical stability have also been proved.[30–32] In the past few years, CP-derived luminescent probes have been widely utilized in super-resolution imaging, multiplexed labelling, fluorescence imaging guided surgery and analysis of disease-related biomarkers.[33–38] In addition, benefitting from the many advantages of CP-based luminescent materials, such as excellent stability, ultra-high brightness and inherent and superior signal amplification capability, a variety of CP-based ratiometric probes have been developed for accurate biomolecule monitoring in a complex biological environment.[39–43]

Professor Li Wu received her PhD degree in Inorganic Chemistry from the Changchun Institute of Applied Chemistry Chinese Academy of Sciences in 2015 under the direction of Professor Xiaogang Qu. She then joined Professor Daniel T. Chiu's research group at the University of Washington (Seattle) as a postdoctoral researcher in 2015. She is now a Professor of the School of Public Health, Nantong University, from 2019. Her research interests focus on the accurate diagnosis and treatment of tumors using functional materials.

Li Wu

Dr Xiaobo Zhou received his MS degree in Optical Engineering from the Nanjing University of Posts & Telecommunications in 2015. He received his PhD degree in Inorganic Chemistry from Fudan University in 2019. He is currently an Associate Professor at the School of Public Health at Nantong University. His research interests are focused on the design and synthesis of luminescent probes and their biomedical applications.
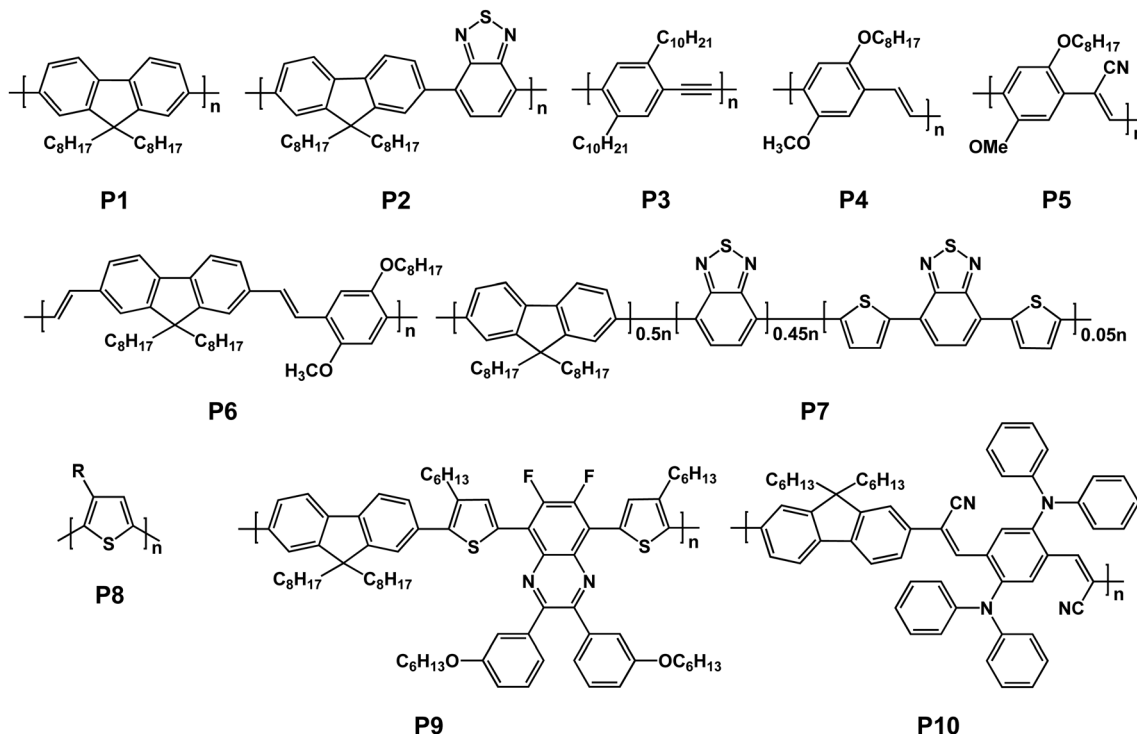
Xiaobo Zhou

Fig. 1 Chemical structures of conjugated polymers.

Table 1 Optical properties of CP-based probes

CPs	$\lambda_{\text{Abs-max}}{}^a$ (nm)	$\lambda_{\text{Em-max}}{}^b$ (nm)	FWHM^c (nm)	Φ^d (%)	τ^e (ns)
P1	380	435	10	40	0.27
P2	450	545	75	7	0.60
P3	390	440	50	12	0.24
P4	485	590	56	1	0.13
P5	494	600	120	60	—
P6	445	510	68	8	0.13
P7	450	650	130	30	4.98
P9	492	652	129	47	1.46
P10	405	673	110	—	—

^{a} Absorption maximum. ^{b} Fluorescence maximum. ^{c} Full width at half maximum. ^{d} Quantum yield. ^{e} Fluorescence lifetime.

This review summarizes the newly achieved progress in the design of CP-based ratiometric luminescent probes and the biosensing performance of these probes *in vitro* or *in vivo*. Herein, we aim to discuss the design principles of CP-derived ratiometric probes and investigate their potential in accurate biomolecule detection. Specifically, the most common types of ratiometric luminescent probes were first introduced. Then, various design principles of CP-based ratiometric biosensors were summarized and compared. Meanwhile, their potential in accurate biodetection in living biosystems was also discussed. Finally, the existing challenges and future prospects of this research field were analyzed. We hope that this review can provide insightful design guidelines and understanding of CP-based ratiometric luminescent probes for future researchers in various disciplinary areas and stimulate more significant academic ideas and clinical applications.
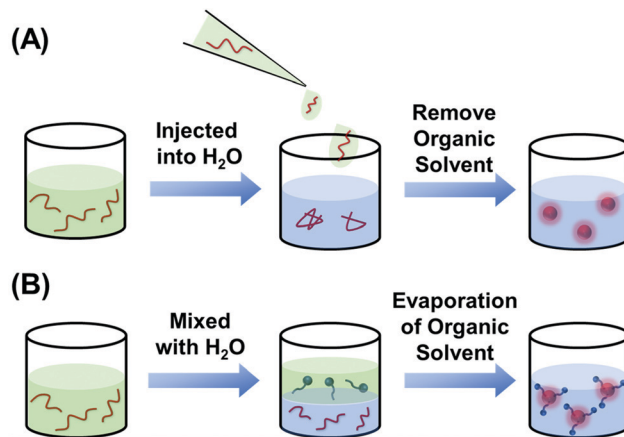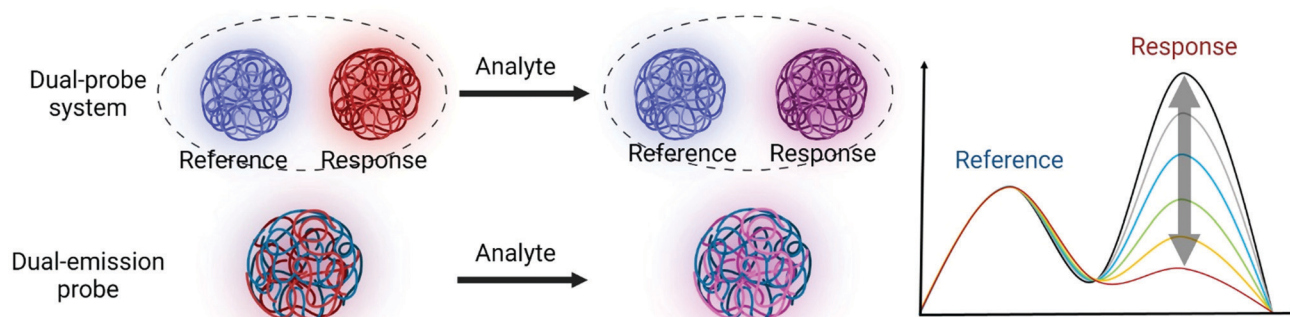

Fig. 2 Schematic illustration of (A) nanoprecipitation and (B) mini-emulsion methods for the preparation of Pdots.

2. Ratiometric fluorescent probes

Ratiometric fluorescent probes in general can be classified into two types according to their target-responsive signal changes (Fig. 3). Type I ratiometric probes are designed with both a target-insensitive emission channel which functions as a built-in reference indicator and a target-sensitive emission channel as the signal sensing reporter to realize ratiometric/colorimetric biosensing. While the construction of type II ratiometric probes is achieved by utilizing two target-sensitive emission channels that exhibit opposite emission signal

This journal is © The Royal Society of Chemistry 2022

J. Mater. Chem. B, 2022, **10**, 7309–7327 | **7311**

Type I : Ratiometric sensing with one stable signal

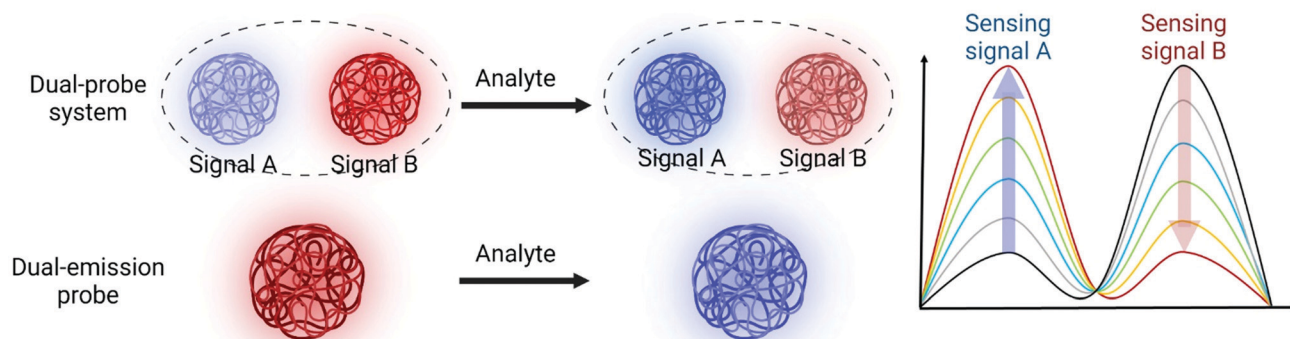## Type II : Ratiometric sensing with two reversible signals

Fig. 3 General principles for the design of ratiometric probes.

variation tendencies in response to the target. The multichannel emission signal could be collected using a single probe or through a combination of two or more entirely independent probes. However, ratiometric sensing platforms with completely independent sensing units may lead to misleading results due to analyte-independent interferences, such as nonspecific binding, instrumental fluctuation, uneven distribution, photobleaching, and variations in the surrounding microenvironment. Therefore, apart from very few ratiometric sensing platforms consisting of two completely independent sensors, ratiometric platforms developed in recent years are mostly presented as a single probe with dual or multiple emission channels, which can efficiently eliminate errors caused by irrelevant factors. In particular, over the past few decades, novel dual-reverse-signal ratiometric probes have gained increasing popularity in the detection and imaging of biomolecules. The common strategy for the fabrication of type II probes is to utilize target-responsive optical influence factors, including, but not limited to charge transfer, proton transfer, energy transfer and chemical reaction. With the addition of analytes, some of the above factors are disturbed, causing reverse signal variations in two or more channels and allowing precise ratiometric determination in complex biological and physiological environments.[44–46] Thus, ratiometric probes with the characteristics of reverse signal variations from dual or multiple channels in response to the target are considered as

favourable candidates in biosensing for their broad dynamic range, high sensitivity and robust reliability.

3. Conjugated polymer-based ratiometric luminescent probes and their applications

3.1 Distance change of energy transfer

In energy transfer systems, efficiency of radiative energy transfer is extremely sensitive to the distance between the donor (D) and the acceptor (A). As a ratiometric luminescent probe constructed using the energy transfer strategy, the energy transfer of the conjugated polymer-based ratiometric luminescent probe is initiated or prevented due to the change in the distance between the D–A pair when exposed to a specific target analyte, resulting in the ratiometric variation of fluorescence signals.

3.1.1 Electrostatic interaction induced distance change. An electrostatic interaction is a common attractive or repulsive interaction between charged molecules, macromolecules, and nanoparticles. Such an interaction-induced distance change between the donor and the acceptor in energy transfer systems are widely utilized to construct ratiometric sensing platforms. Because of the presence of π-conjugated repeat units in CPs, the energy can be transferred efficiently from CPs to neighbouring
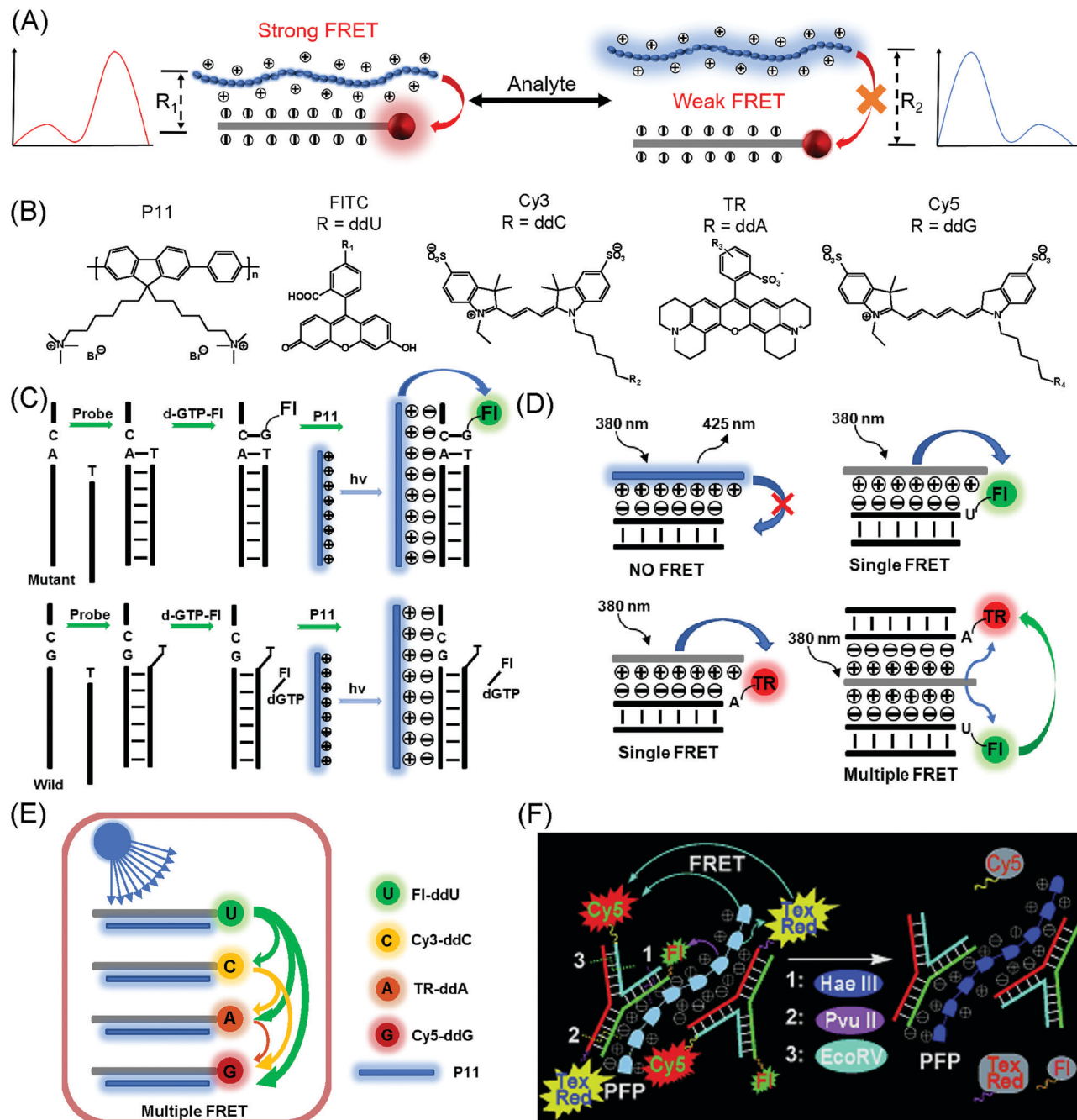
7312 | *J. Mater. Chem. B*, 2022, **10**, 7309–7327

This journal is © The Royal Society of Chemistry 2022

Fig. 4 (A) Design strategies for ratiometric probes based on the electrostatic interaction-induced distance change between an energy donor and acceptor. (B) Chemical structures of the energy donor (P11) and energy acceptor (organic fluorescent dyes: FITC, Cy3, TexRed and Cy5) used in these assays. A schematic diagram of the detection of (C) single nucleotide mutations, (D) double nucleotide mutations, (E) multiple nucleotide mutations and (F) nucleases. Reproduced with permission from ref. 50. Copyright 2009 Wiley-VCH.

luminophores which possess an appropriate spectral overlap and a dipole orientation with CPs, resulting in amplified luminescence signals from the neighbouring luminophores. If the added analyte can cause the distance change between the CPs and the luminophores, analyte-dependent variations of reverse luminescence signals attributed to the CPs and the luminophores respectively would be obtained (Fig. 4A).

Based on this strategy, Duan *et al.* by using conjugated polymers P11 proposed a series of highly sensitive ratiometric

detection approaches for DNA mutation analysis. In the design of these approaches, the positively charged quaternary ammonium group was conjugated on the side chains of CPs to serve as the light-harvesting antenna and energy transfer donor, while the negatively charged single-chain DNA fragment (part of the p53 exon) was used as the receptor of the target. Finally, fluorescent organic dyes (fluorescein, Cy3, TexRed and Cy5, see Fig. 4B) were introduced as the energy transfer acceptor by DNA extension reactions.[47] As shown in Fig. 4C, the mutant target

This journal is © The Royal Society of Chemistry 2022

J. Mater. Chem. B, 2022, **10**, 7309–7327 | **7313**

DNA had a mutation site on the nucleotide guanine (G) (replaced by adenine), and a receptor DNA fragment with thymine (T) at 3' termini was designed as a complementary probe to recognize the mutant target DNA fragment. The fluorescein-labelled dGTP was used in specific fluorescent labelling of the fully complementary co-ordinated mutant DNA by C–G base coordination. Upon the addition of P11, the strong electrostatic interaction between the co-ordinated mutant DNA and P11 causes a decrease in the distance between them and shortened the distance between P11 and the labelled fluorescein, which resulted in the ratiometric variation of the fluorescence signals. In contrast, due to the double-stranded DNA fragments generated from the complementary coordination of the wild-type DNA, it was difficult to label the designed receptor DNA with dGTP–fluorescein. The distance between P11 and the labelled fluorescein could not be narrowed down even when the DNA and P11 were close enough to each other. Therefore, with the existence of the wild-type DNA, the fluorescence signals of both P11 and fluorescein did not vary. Under the conditions of such probes and detection strategy and an excitation wavelength of 380 nm, the ratiometric signal change ($I_{\text{fluorescein}}/I_{\text{P11}}$) in the presence of mutant-type DNA was 8 times that of wild-type DNA. Moreover, it is noticeable that the allele frequency that this probe was able to detect was as low as 2%. Based on these observations in this study, this strategy had been further applied to the detection of dual and multiple gene mutations through the utilization of the multistep fluorescence resonance energy transfer (FRET) from CPs to fluorescent dyes (see Fig. 4D and E).[48] As shown in Fig. 4E, different bases with a specific co-ordinate to the neighbouring sites of the mutant site of the target DNA were labelled with different fluorophores of different emission colours. Uracil (U) was labelled with green emissive fluorescein, cytosine (C) with orange emissive Cy3, adenine (A) with red emissive TR, and guanine (G) with NIR emissive Cy5. The mechanism of using receptor DNA fragments for mutant-type DNA recognition was similar to previous studies, and what differed from other studies was the readout method of the fluorescence signal of the detection results. In this work, upon the addition of P11, the electrostatic interactions between P11 and fluorophore labelled DNA would lead to a multistep-FRET process. By collecting and analysing the fluorescence change of multiple emission channels and calculating the FRET efficiency of the energy transfer system including CPs and different fluorophores, multiple DNA mutations can be detected simultaneously.

Then, adopting such a multiplexed detection strategy, Zhang et al. further ameliorated the data analysis method and applied this approach to clinical sample detection, which demonstrated the prospects of this approach in the practical application of cancer diagnosis.[49]

Moreover, according to the reverse process of the above-mentioned principles being used in multiple DNA mutation detections, P11 was also adopted in the multiplexed detection of endonuclease.[50] As shown in Fig. 4F, the endonuclease sensing platform was constructed with the cationic P11 being used as the energy donor and Y-shaped DNA (Y-DNA) labelled with three types of fluorophores (fluorescein, TexRed and Cy5) as the energy acceptor and endonuclease receptor. In this work, the characteristic design principle was that the fluorescents labelled with fluorescein, TexRed, and Cy5 respectively were separately linked at the 5′-termini of different branches in one single Y-DNA, and that each branch of Y-DNA included a nuclease cleavage site. Under the condition of mixing P11 and Y-DNA in an aqueous solution without nuclease, they were in proximity to each other under the drive of strong electrostatic interactions, which allowed the cascade energy transfer between P11 and different fluorophores, generating multiple emission bands. While in the presence of a single kind of target nuclease, the corresponding DNA fragment carrying the fluorophore was generated and the Y-DNA was left away, thus leading to a sharply decreasing fluorescence signal from such fluorophores and changes in other emission channels. Based on the multiple changes in the fluorescence signals from different fluorophores, the type and content of target nucleases can be identified and calculated. With the treatment of double or triple kinds of nucleases, the complexity of the fluorescence spectral change of the probes dramatically increased. Analysis of multiple nucleases was performed by logic gates. Because of properties such as high sensitivity, convenience, and low cost, the ratiometric fluorescence detection approach on the basis of an energy transfer system where CPs were used as the donor units has been widely employed in the detection of proteins,[51–54] regulatory peptide,[55] adenosine deaminase[56] and other gene mutations.[57–59]

The strategy based on analyte-induced energy transfer from CPs to other fluorophores for ratiometric fluorescent probe construction has achieved much progress so far. Another strategy on the basis of analyte-induced energy transfer among CPs themselves has also been adopted to construct ratiometric probes for biomolecule detection. According to the design principles of the backbone and side-chain structure of CPs, a series of highly sensitive and reliable luminescent probes were successfully developed for the ratiometric detection of heparin, a kind of negatively charged mucopolysaccharide which plays a pivotal role in the regulation of various physiological processes (Fig. 5).[60] In these studies, the response mechanism of CP-based probes for heparin detection is summarized in Fig. 5A. The probes were developed by modifying the cationic groups on the side chains of traditional CPs. Thus, in the presence of heparins, the CP-based probes were aggregated to each other, which could be attributed to the strong electrostatic interactions between positively charged CPs and negatively charged heparins (Fig. 5A). The aggregation of CPs could shorten the distance between different CPs in aqueous solution, and when energy transfer occurs intra-CPs or inter-CPs, such heparin-induced aggregation of CPs will generate the ratiometric variation of the fluorescence signal of CPs.

For example, Liu et al. first demonstrated the potential of cationic CP-based "turn-on" probes for heparin detection, in which the aggregation-induced hydrophobic microenvironment of CPs enhanced their fluorescence. Then, other more studies further optimized this strategy and enabled label-free,
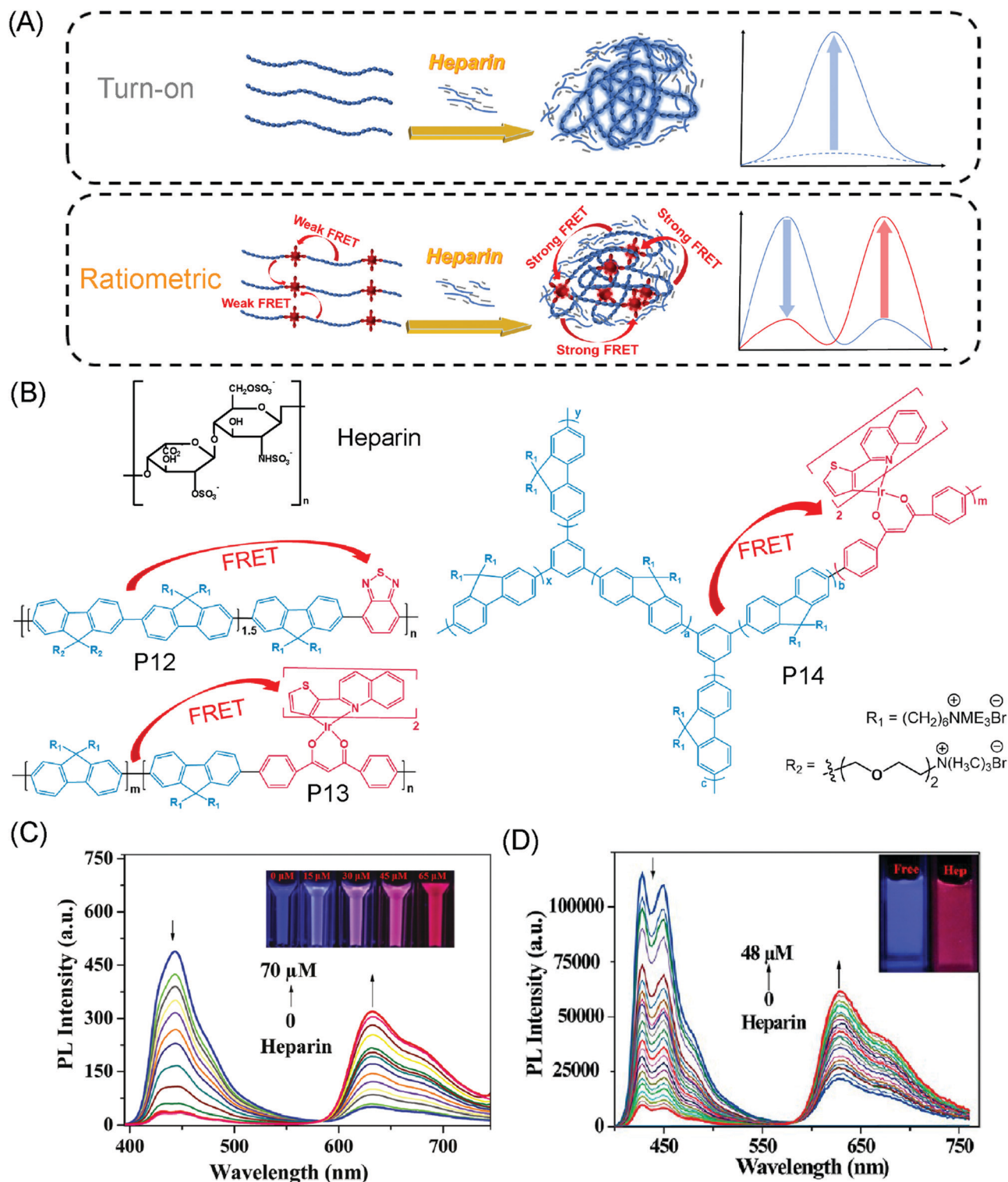
7314 | J. Mater. Chem. B, 2022, 10, 7309–7327

This journal is © The Royal Society of Chemistry 2022

Fig. 5 (A) Schematic illustration of the response mechanism of CP-based singe/dual-emissive probes for heparin sensing. (B) Chemical structures of heparin and dual-emissive CP-based heparin-sensitive probes. (C) PL spectra of the heparin-sensitive probe P13 in HEPES buffer with the concentration of heparin from 0 to 70 μM upon excitation at 380 nm. Inset: Emission color changes of solution excited at 365 nm. Reproduced with permission from ref. 39. Copyright 2013 Wiley-VCH. (D) PL spectra of the heparin-sensitive probe P14 in HEPES buffer with the concentration of heparin from 0 to 48 μM upon excitation at 380 nm. Inset: emission color changes of solution excited at 365 nm. Reproduced with permission from ref. 67. Copyright 2013 American Chemical Society.

This journal is © The Royal Society of Chemistry 2022

J. Mater. Chem. B, 2022, 10, 7309–7327 | 7315

quantifiable and visual detection of heparin.[61–64] Since that these developed CPs mostly included only one kind of repeat unit in the backbones of CPs, these CPs could only emit a single emission band, which was not favourable for constructing heparin-sensitive ratiometric fluorescent probes. According to these results, the authors of these studies further designed cationic CPs (P12, Fig. 5B) which contained two different repeat units (*i.e.*, polyfluorene unit and polyfluorene–benzothiadiazole unit) for heparin sensing.[65,66] Due to the spectral overlap between covalent-linked polyfluorene and polyfluene–benzothiadiazole, energy transfer from polyfluorene to polyfluorene–benzothiadiazole was made possible. Interestingly, the efficiency of such an energy transfer system was significantly affected by the aggregation degree, which might be attributed to not only the aggregation of CPs, but also the buckling of a single CP molecule since the former would result in the intermolecular stacking of CPs and both the former and the latter could shorten the distance between polyfluorene (the donor) and polyfluorene–benzothiadiazole (the acceptor). Without heparins and since that P12 is water-soluble, conjugated polymers would largely maintain the single molecular state and exhibit inefficient energy transfer from polyfluorene to polyfluene–benzothiadiazole, leading to a pure blue fluorescence with almost no obvious emissions over 500 nm. Upon the addition of heparin, due to the heparin-induced aggregation of P12, an orange emission was gradually enhanced at the expense of the blue emission. Therefore, according to the reverse variation of emissions at 420 nm and at 600 nm with the addition of heparins, the ratiometric fluorescence detection of heparin was realized.

Furthermore, to achieve time-resolved luminescence sensing and fluorescence lifetime imaging, Shi *et al.* reported a novel heparin-sensitive phosphorescent conjugated polyelectrolyte (PCPE) with a long emission lifetime.[39] They covalently introduced the phosphorescent Ir(III) complexes to the backbone of polyfluorene and obtained cationic dual emissive P13. Due to the large spectral overlap between the polyfluorene and Ir(III) complexes, an energy transfer system was constructed using polyfluorene as the donor and Ir(III) complexes as the acceptor. In an aqueous solution without heparin, the emission spectrum of the free probe solution was dominated by the fluorescence of polyfluorene at 440 nm, and the phosphorescence emission from Ir(III) complexes was negligible. With the addition of heparin, the red phosphorescence emission intensity at 630 nm was dramatically enhanced, which could be attributed to the heparin-induced aggregation of P13 (Fig. 5C). Using this ratiometric probe, quantification of heparins in the range of 0–5 μM in the serum was realized. Meanwhile, with the advantages of the long lifetime of the emission signal from Ir(III) complexes, the capacity of such probes for heparin detection in complicated environments such as clinical blood samples was confirmed using the time-resolved photoluminescence imaging technique. Furthermore, such a design principle for constructing switchable CP-based fluorescence/phosphorescence luminescent probes had artfully combined the signal amplification effect of CPs and the long lifetime of phosphorescence Ir(III) complexes, which made it possible to use the probes in ratiometric detection and time-resolved detection simultaneously and to obtain more accurate, reliable and sensitive results of analyte detection.

Nevertheless, concerning the aggregation-induced quenching (ACQ) effect of luminescent CPs with traditional linear backbone structures, they then developed a kind of hyper-branched conjugated polymer (HCP) with a 3D topology structure to reduce the ACQ effect of CPs. By adopting this strategy, fluorescence/phosphorescence dual emissive HCPs (P14) were designed and applied to build a well-performed sensing platform (Fig. 5D).[67] In a similar way, such a strategy for constructing CP-based ratiometric luminescent probes has also demonstrated its potential to be used in the detection of ATP[68,69] and bacterials.[70,71]

3.1.2 Hydrophilic/hydrophobic interaction induced distance change. The strategy of the ratiometric CP-based luminescent probe construction on the basis of the electrostatic interaction-induced distance change between the donor and the acceptor in an energy transfer system has achieved great progress. However, when the target analytes could not induce considerable electrostatic interactions among the CP probes themselves or between the CP probes and other luminescent reporters, the utilization of the electrostatic interaction-based strategy for constructing ratiometric luminescent CP probes for the detection of biomolecules was invalid. Therefore, according to other intermolecular interactions between the CP-based probe and the analytes, the CP-based ratiometric probes constructed based on the analyte-induced distance change in the energy transfer process had also been developed.

According to the hydrophobic–hydrophobic interaction-induced distance change in the energy transfer process in CP-based probes, Kuo *et al.* reported polyacetylene-modified Pdots for the ratiometric detection of Pb^{2+} (Fig. 6).[72] Two different fluorescent and hydrophobic units (*i.e.*, P15 and NIR695) were encapsulated by 15-crown-5 and carboxyl-functionalized diacetylene to form water-dispersed Pdots, which can sandwich coordinated to Pb^{2+} selectively. Meanwhile, the derivatives of diacetylene could be further polymerized for the formation of polydiacetylenes, which could seal the doped luminophore NIR695 (Fig. 6A). A highly efficient energy transfer process occurred in this nanosystem because of the spectral overlap between the emission of P15 and the absorption of NIR695. Upon the addition of Pb^{2+}, sandwich complexes formed and the conjugation of polydiacetylenes were shortened, accompanied by the leaching of NIR695 dyes. The fluorescence intensity from the polymer at 650 nm increased at the expense of NIR dyes decrease at 715 nm (Fig. 6B), and the colour change of the solution was clearly visible (photograph at the top of Fig. 6C). Besides, as shown in Fig. 6C, the sensing platform exhibited great selectivity for Pb^{2+}. However, poor stability and dye leakage might lead to misleading conclusions, thus hindering the application of the ratiometric probe developed in this work.

Based on the supramolecular interaction, Wang *et al.* developed functionalized Pdots and fluorescent dyes co-assembled the supramolecular ensemble. By utilizing the
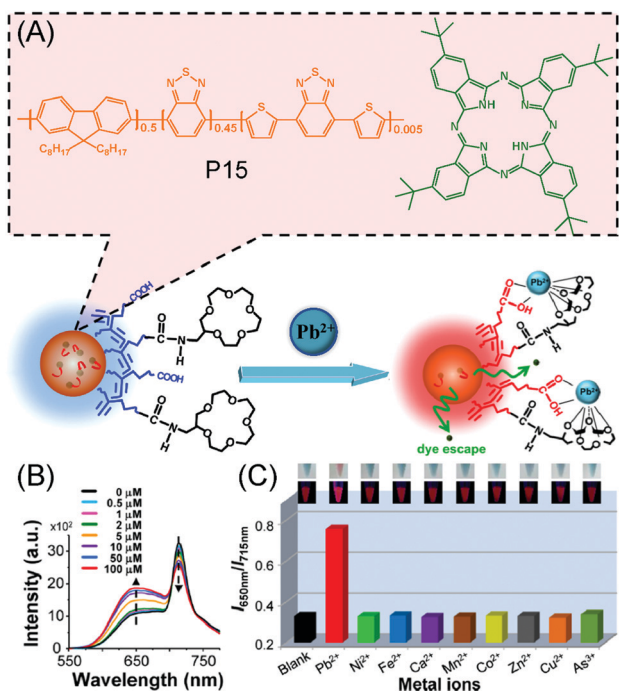
7316 | *J. Mater. Chem. B*, 2022, **10**, 7309–7327

This journal is © The Royal Society of Chemistry 2022

Fig. 6 (A) Schematic diagram of the construction of the CP-based Pb^{2+} sensing probe. (B) Emission spectra of Pdots under different concentrations of Pb^{2+}. The concentration range of Pb^{2+} is 0 to 100 μM (λ_{ex} = 450 nm), disposed with 20 nM Pdots at pH 7.4. (C) The effect of different ionic species (50 μM) on the luminescence intensity of Pdots solution. Inset: each sample under bright field (upper row) and UV light at 365 nm (lower row). Reproduced with permission from ref. 72. Copyright 2015 American Chemical Society.

stronger selective interaction between the target analyte lectin and the designed fluorescent dyes, the dissociation of the dyes from the ensemble occurred, which then realized the selective ratiometric fluorescence detection of lectin.[40] As shown in Fig. 7A, in such a supramolecular ensemble, blue-emitting Pdots (PFO-Pdots) were used as the energy transfer donor and the red-emitting glycol-modified organic dyes as the energy transfer acceptor. Due to the close distance between PFO-Pdots and glycol-modified dyes in the supramolecular ensemble, an efficient energy transfer from PFO-Pdots to the dyes occurred, resulting in a strong red emission of the supramolecular ensemble with the excitation of PFO-Pdots. In the presence of lectin, as the intermolecular interaction between glycol-modified dyes and lectins was stronger, glycol-modified dyes were dissociated to PFO-Pdots, thus increasing the distance between the donors and the acceptors in this energy transfer system. Compared with other techniques, such as zeta potential analysis, transmission electron microscopy (TEM) and dynamic light scattering (DLS) that have been used to measure the content of lectins, the approach of the ratiometric detection technique developed in this work exhibited the ability to detect lectins in a more complicated environment. This strategy was further applied to the exploration and blocking of human-infecting influenza viruses.[73]

With combined interactions including the above-mentioned intermolecular interaction (*i.e.*, electrostatic interaction and

hydrophobic–hydrophobic interaction) and the rigidity of the molecule-induced distance change between the donor and the acceptor in an energy transfer system, CP-based probes used in the ratiometric sensing of the conformation of calmodulin (CaM) were developed. Calmodulin (CaM) is a multifunctional intermediate calcium-binding messenger protein expressed in eukaryotic cells.[74] As shown in Fig. 7B, under the existence of Ca^{2+}, the conformation of CaM changes from the closed configuration to the open state and is accompanied by the change of enhanced hydrophobicity and decreased negative charges.[75] In this work, CaM was labelled with an enhanced green fluorescent protein (EGFP), which is convenient for constructing an energy transfer system and used as the acceptor. The cationic water-soluble CPs (P11) were designed as the donor in such an energy transfer system, and amphiphilic graphene oxide (GO) used for the fluorescence quenching of the EGFP and for the capture of hydrophobic groups.[76] The ratiometric sensing platform is composed of a hybrid system by these constituents. The sensing mechanism of such an approach is shown in Fig. 7B, and with the absence of Ca^{2+}, the EGFP labelled CaM (EGFP-CaM) was retained at the close configuration, which exhibits poor-hydrophobicity and a sufficient negative charge. Owing to the strong electrostatic interaction shortening the distance between P11 and EGFP-CaM while lengthening the distance between EGFP-CaM and GO, an efficient energy transfer from cationic P11 to EGFP occurred and the fluorescence quenching effect of GO to EGFP-CaM was reduced based on the large spectral overlap of P11 and EGFP. Therefore, in such a situation, the green emission attributed to the fluorescence of EGFP was dominated in the hybrid system. Upon the addition of Ca^{2+}, the flexible EGFP-CaM will be binding with them and get converted to a long and rigid helix EGFP-CaM/Ca^{2+}, exhibiting less negatively charged surfaces and enhanced hydrophobicity and rigidity. Such a property change, as compared to those of EGFP-CaM/Ca^{2+} to EGFP-CaM, produces the enhanced hydrophobic–hydrophobic interaction between EGFP-CaM/Ca^{2+} and GO, and weakened electrostatic interaction between EGFP-CaM/Ca^{2+} and P11. Therefore, compared with that in EGFP-CaM, the distance between EGFP and GO was shortened, while the distance between EGFP and P11 was lengthened, resulting in the decreased energy transfer efficiency from P11 to EGFP and the enhanced fluorescence quenching effect of GO to EGFP. So, in the presence of Ca^{2+}, the fluorescence of this sensing platform was dominated by the emission of P11. Very interestingly, according to this approach, the conformation of CaM can be reversibly and quantitatively visualized by monitoring the ratiometric fluorescence variation, and it is workable for calmodulin to induce the transformation *in vivo*.

3.2 Chemical change of energy transfer acceptors

It is well known that the efficiency of the energy transfer process mainly depends on the distance, the spectral overlap and the dipole orientation between the donors and the acceptors. Apart from designing the CP-based ratiometric luminescent probe on the basis of the distance change in energy

This journal is © The Royal Society of Chemistry 2022

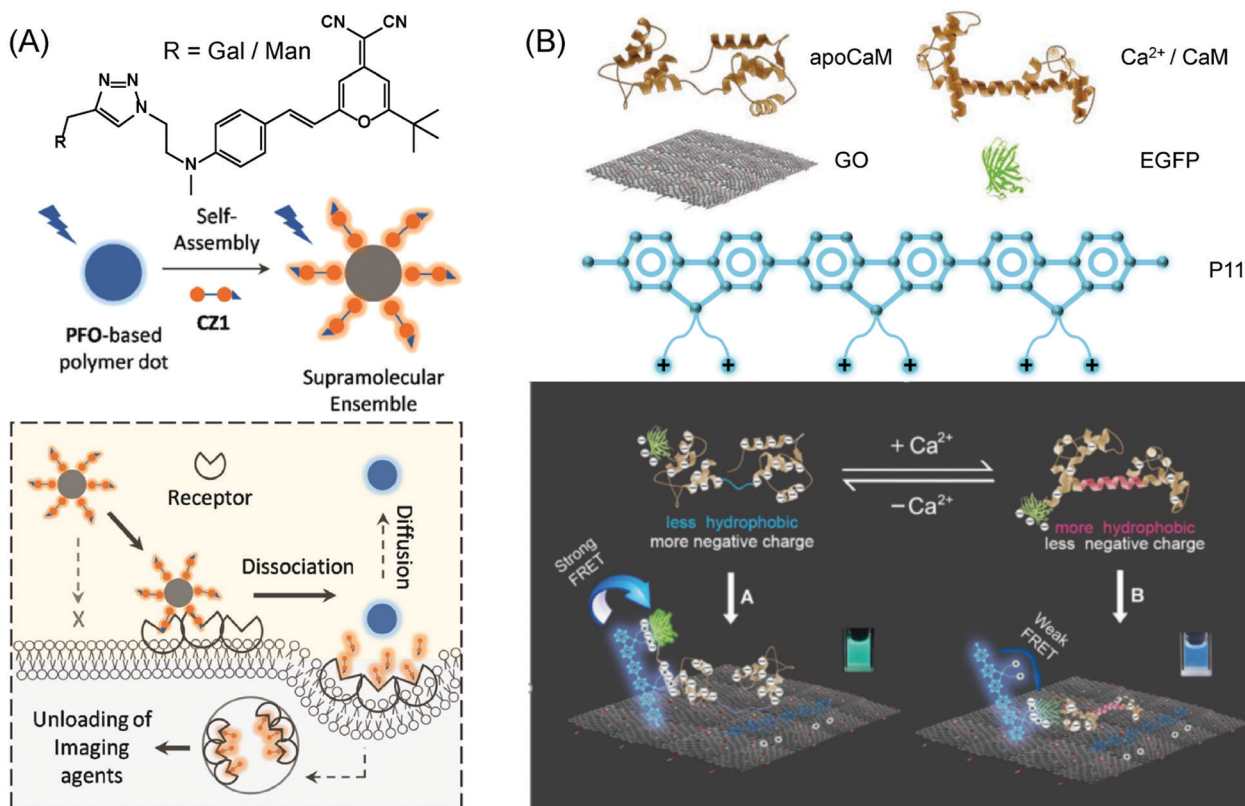*J. Mater. Chem. B*, 2022, **10**, 7309–7327 | **7317**

Fig. 7 (A) Schematic representation of nanoprobe self-assembly and receptor-controlled targeted delivery of imaging agents. Reproduced with permission from ref. 40. Copyright 2017 American Chemical Society. (B) Schematic illustration of the GO-CP-based hybrid probe for detecting Ca²⁺-induced conformational changes of CaM. Reproduced with permission from ref. 76. Copyright 2015 Wiley-VCH.

transfer, analyte-induced alternations of the spectral overlap between the donors and the acceptors in the energy transfer system were also demonstrated to act as an effective strategy. Considering that the spectra of luminophores mostly depend on their structure, thus alternations of the spectral overlap between the donors and the acceptors in fact were mainly caused by the analyte-induced chemical change of the acceptors. In general, to construct dual or multiple luminescent center-contained CP-based probes, CPs featured with light-harvesting and signal amplification were designed as the energy transfer donor in order to enhance the sensitivity of ratiometric detection. Therefore, the strategy for designing the ratiometric CP-based probes discussed in this section mainly utilized the analyte-induced chemical change of the acceptors to generate the ratiometric variation of the fluorescence signal.

The H_2O_2-mediated oxidation of aryl boronates to phenols has been widely used in constructing H_2O_2-sensitive probes.[77] With advantages from the outstanding signal amplification properties of CPs, various ratiometric fluorescent probes constructed using the hybrid CPs as the donor and H_2O_2-response probe as the acceptor were developed. For example, He *et al.* developed a ratiometric CP-based probe for H_2O_2 detection by covalently linking the H_2O_2-responsive boronate-protected fluorescein on the side chains of blue-emitting polyfluorene (Fig. 8). With the absence of H_2O_2 and since that colourless

boronate-protected fluorescein is almost non-emissive, energy cannot be transferred from CPs to boronate-protected fluorescein, although the distance between CPs and colourless fluorescein was close enough. Then, in such a situation, the probe exhibited only a strong blue emission at 420 nm. With the presence of H_2O_2, the boronate-protected fluorescein was converted to fluorescein accompanied by an extremely enhanced absorption band at 490 nm and an emission band at 520 nm. Therefore, efficient energy transfer from CPs to fluorescein occurred, which lead to a decreased emission at 440 nm and an increased emission at 520 nm. In addition, since this generation of H_2O_2 can be induced by glucose oxidase-catalysed reactions, such ratiometric probes were further applied to the convenient and quantitative detection of glucose. Similarly, it was found that such H_2O_2-sensitive ratiometric fluorescent probes had also been successfully used as the signal transducer of respective substrates or enzymes.[78]

Different from the above-mentioned mechanism of hydrogen peroxide detection, the pH-induced chemical change of probes is reversible. Numerous smart construction strategies for optical pH sensors have been reported over the past decades.[79–81] In 2011, Chan *et al.* first proposed dual-emissive Pdots for ratiometric pH sensing.[82] In their work, the pH-insensitive P3 was used as the donor and the pH-sensitive fluorescein derivative as the acceptor in the energy transfer
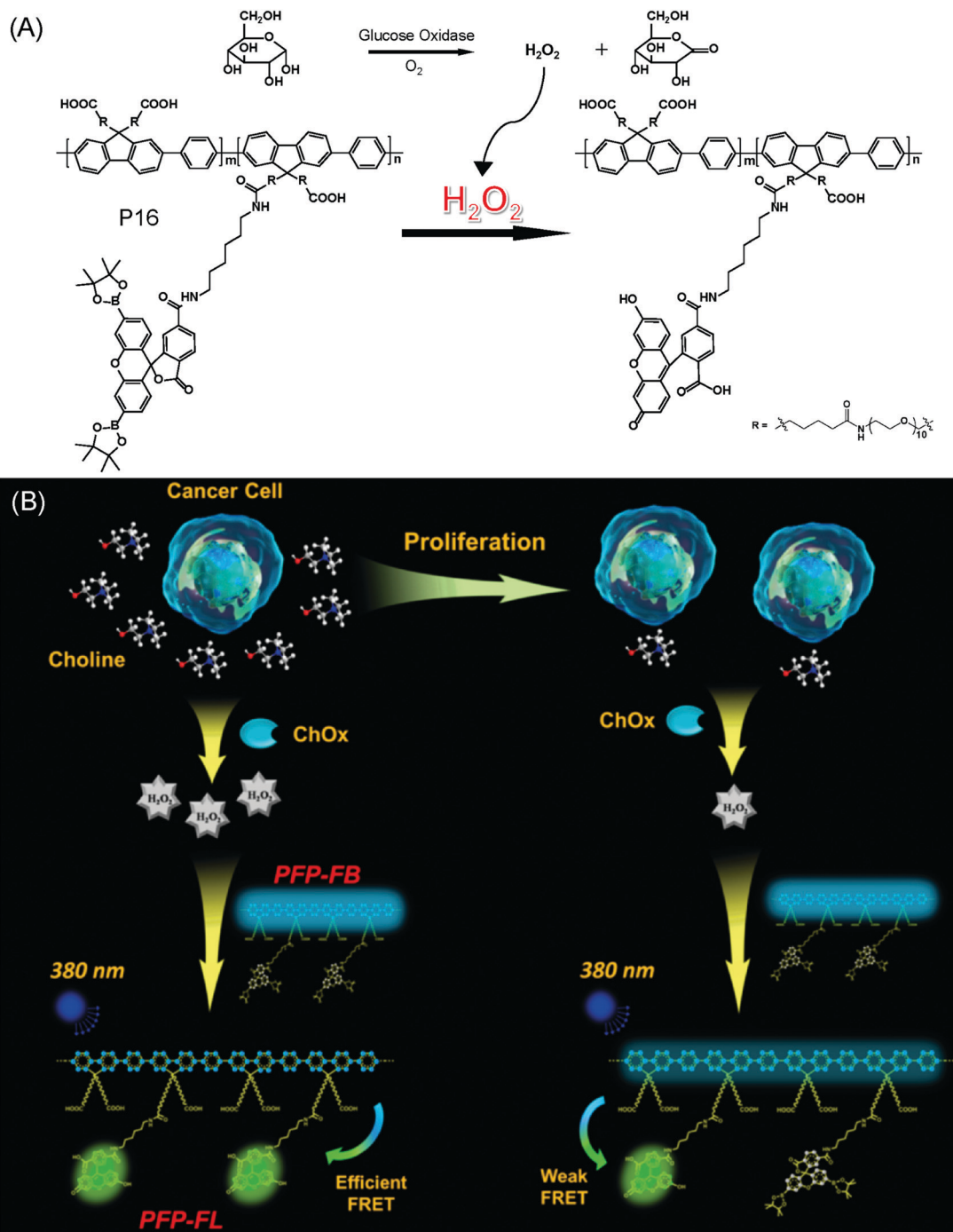
Fig. 8 Schematic illustration of H_2O_2-sensitive probes in the monitoring of (A) aerobic oxidation reactions and (B) the process of choline depletion in living cells. Reproduced with permission from ref. 78. Copyright 2015 American Chemical Society.

system (Fig. 9A). Due to the deprotonation of the pH-sensitive fluorescein, the fluorescence intensity at 515 nm enhanced gradually with an increase in pH, while the fluorescence intensity from P3 at 440 nm was kept constant. The ratio of the emission intensity of the conjugated polymer and fluorescein changed linearly and reversibly. In addition, a near-infrared squaraine derivative dendronized by steric carbazole groups was covalently incorporated into the backbone of

polyfluorenes to construct a dual emissive Sq-Pdot for ratiometric pH sensing.[41] As shown in Fig. 9B, in a basic or neutral environment, due to the energy transfer from the polyfluorene backbone to squaraines, a strong NIR fluorescence peak at 700 nm which belonged to squaraines was observed with the excitation of polyfluorene. Conversely, in an acidic environment, squaraines were protonated and accompanied by a decreased fluorescence peak at 700 nm. Due to the fewer
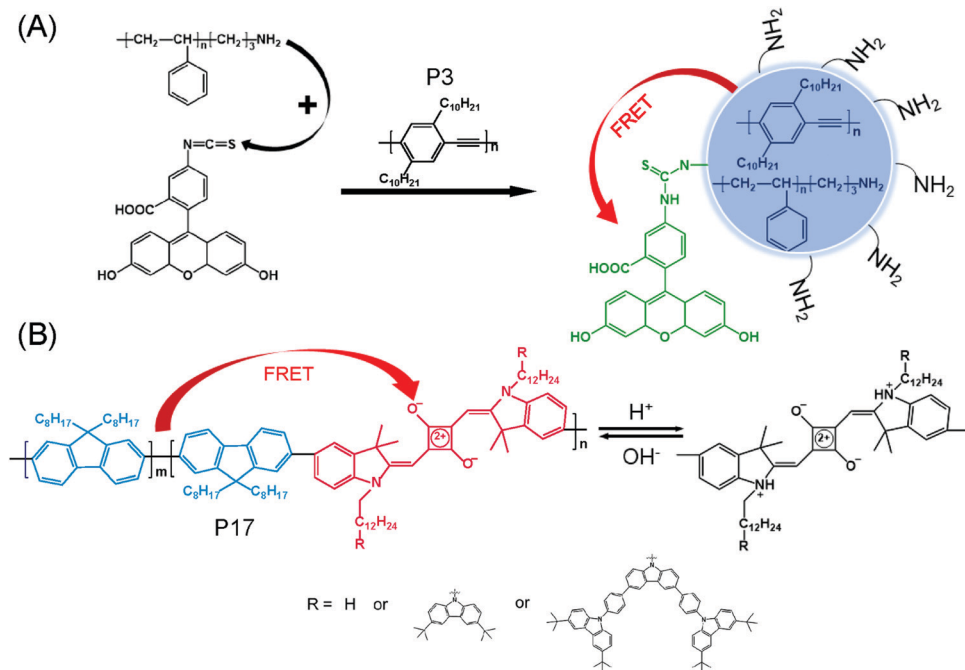
This journal is © The Royal Society of Chemistry 2022

J. Mater. Chem. B, 2022, 10, 7309–7327 | 7319

Fig. 9   (A) The construction principle of pH-sensitive Pdot bases on P3. (B) Chemical structure of P17 and mechanism for ratiometric pH sensing.

variations of the absorption spectra of squaraines at different pH environments, the efficiency of the energy transfer process in this designed probe at different pH environments was quite close. Therefore, with different pH values, the intensity of emission from polyfluorene at 440 nm was kept constant, while the intensity of emission from squaraines at around 700 nm varied obviously, indicating the excellent pH sensitivity of such a designed probe in both acidic and basic solutions. In addition, cellular experiments showed that these Pdots have comparable pH sensitivity to the commercially available pH sensing probe SNARF-1, demonstrating the prospects of the probe in practical applications. Such matrix networks were assumed to provide little protection against uninterested factors. To overcome the potential leakage and bleaching, core–shell structures were introduced to fabricate pH-sensitive ratiometric nanoprobes which allowed the separation of luminophores in order to achieve better pH-sensing performance.[83] Based on the above-described studies, the second analyte-sensitive unit was also further introduced into the pH sensing platform, such as Cu^{2+}-sensitive or oxygen-sensitive units, making it possible to conduct simultaneous sensing of the two analytes.[84,85]

Bioactive species, including reactive oxygen species (ROS), reactive nitrogen species (RNS), reactive sulfur species (RSS), CO, ATP and so on, can also lead to alternations of the chemical structure of luminescent probes.[86–90] About this, Pu *et al.* developed a CP-based ratiometric probe for RONS sensing.[91] As shown in Fig. 10A, NIR-emissive P10 was chosen as the signal transducer, and the IR775COOH that was reported to be degraded by RONS was conjugated to the surface of Pdots through a coupling reaction activated by carbodiimide.[92] Without RONS, energy can be transferred from Pdots to the cyanine
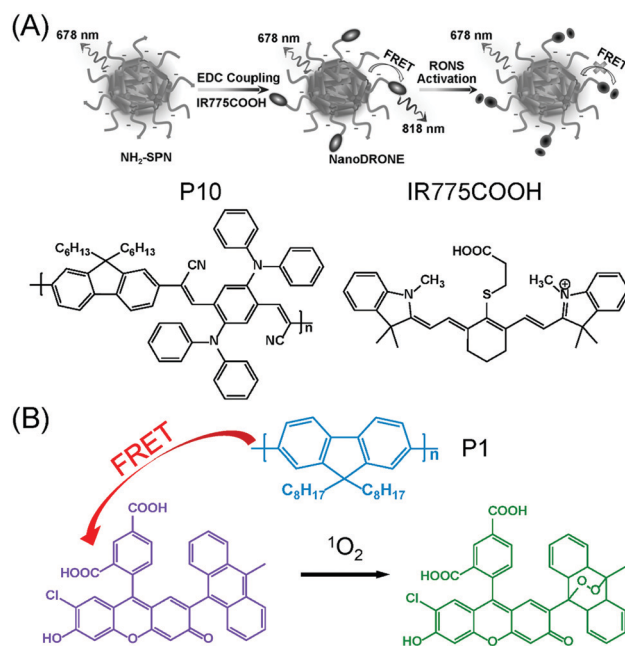

Fig. 10   (A) Preparation of the RONS-sensitive nanoprobe and chemical structures of P10 and IR775COOH. Reproduced with permission from ref. 91. Copyright 2013 Wiley-VCH. (B) Illustration of the sensing mechanism using the CP-based singlet oxygen sensing probe.

dye derivative. With an increase in the concentration of RONS, the fluorescence emission at 678 nm contributing to P10 increased at the expense of the emission at 818 nm. Further experiments *in vivo* were carried out, and it was confirmed that the proposed dual-emitting Pdots could be employed to

7320 | *J. Mater. Chem. B*, 2022, **10**, 7309–7327

This journal is © The Royal Society of Chemistry 2022

monitor RONS in cells and small animals. Similarly, Hou *et al.* prepared singlet oxygen sensor green (SOSG)-doped Pdots for the sensitive detection of singlet oxygen.[93] The $^1O_2$-insensitive ultra-bright CP (P1) was used as the energy transfer donor, and the $^1O_2$-sensitive SOSG was used as the energy transfer acceptor and the responsive group of this probe (Fig. 10B). With the increased concentration of $^1O_2$, the emission intensity at 530 nm was enhanced, while the emission intensity at 436 nm kept stable together with a significant enhancement of I_{530}/I_{436}. Fluorescence imaging in living cells was carried out, and the potentiality of the probe in the detection of intracellular $^1O_2$ was confirmed.

However, sensing probes based on these strategies may suffer from drawbacks regarding photo- and chemistabilities. Taking this issue into consideration, Wu *et al.* developed a polymer-based all-in-one probe for HOCl sensing.[42] As illustrated in Fig. 11A, ClO$^-$-insensitive component benzoxadiazole (OBT) was used as the energy donor and 4,7-bis(2-thienyl)-2,1,3-benzoselenadiazole (SeTBT) sensitive to ClO$^-$ was used as the energy acceptor. Without ClO$^-$, energy was allowed to be transferred from OBT to SeTBT efficiently. With the increase in the concentration of ClO$^-$, the energy acceptor SeTBT was oxidized and the fluorescence intensity at 680 nm (attributed to SeTBT) decreased dramatically accompanied by the
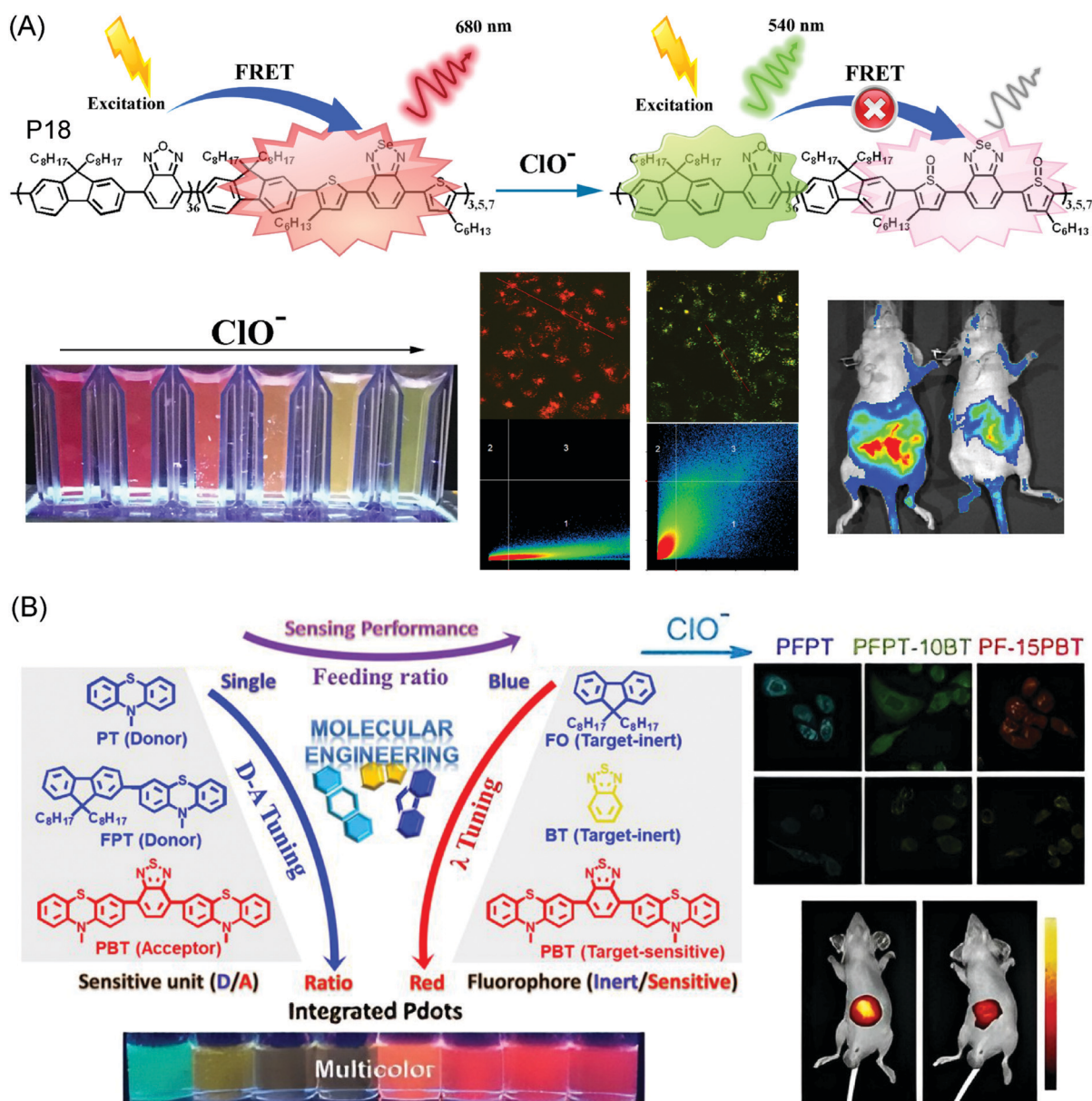

Fig. 11 (A) Ratiometric hydrocholorous acid sensing platform based on all-in-one fluorescent CPs and the images of probes for detecting ClO$^-$ both *in vitro* and *in vivo*. Reproduced with permission from ref. 42. Copyright 2017 American Chemical Society. (B) Schematic illustration of the design strategy of a series of all-in-one HOCl-sensitive probes based on CPs for *in vitro* and *in vivo* imaging. Reproduced with permission from ref. 94. Copyright 2021 American Chemical Society.

This journal is © The Royal Society of Chemistry 2022

J. Mater. Chem. B, 2022, **10**, 7309–7327 | **7321**

enhancement of the emission intensity at 540 nm (attributed to OBT).

Meanwhile, the fluorescence colour of the solution changed from red to orange and finally to green with the increased concentration of ClO⁻. Additionally, the probe was further applied in monitoring of hypochlorous acid fluctuations in macrophage cells and in peritonitis imaging in living mice, suggesting the excellent biocompatibility and high physiological stability of the probe. Similarly, Zhang *et al.* designed and synthesized a series of ClO⁻-sensitive single-component fluorescent probes, which provided a universal strategy for

designing all-in-one CPs and Pdots through molecular engineering (Fig. 11B).[94]

3.3 Photochemical change of the energy transfer acceptors

In addition to the strategies based on perturbations of the intra/inter-molecules energy transfer by changing the chemical structure of probes, the analyte-induced photochemistry change was also utilized to construct CP-based ratiometric luminescent probes. The latter strategy lies on the direct energy transfer process between one kind of the repeat units in the CPs and the analytes or the substrate and the generator of analyte
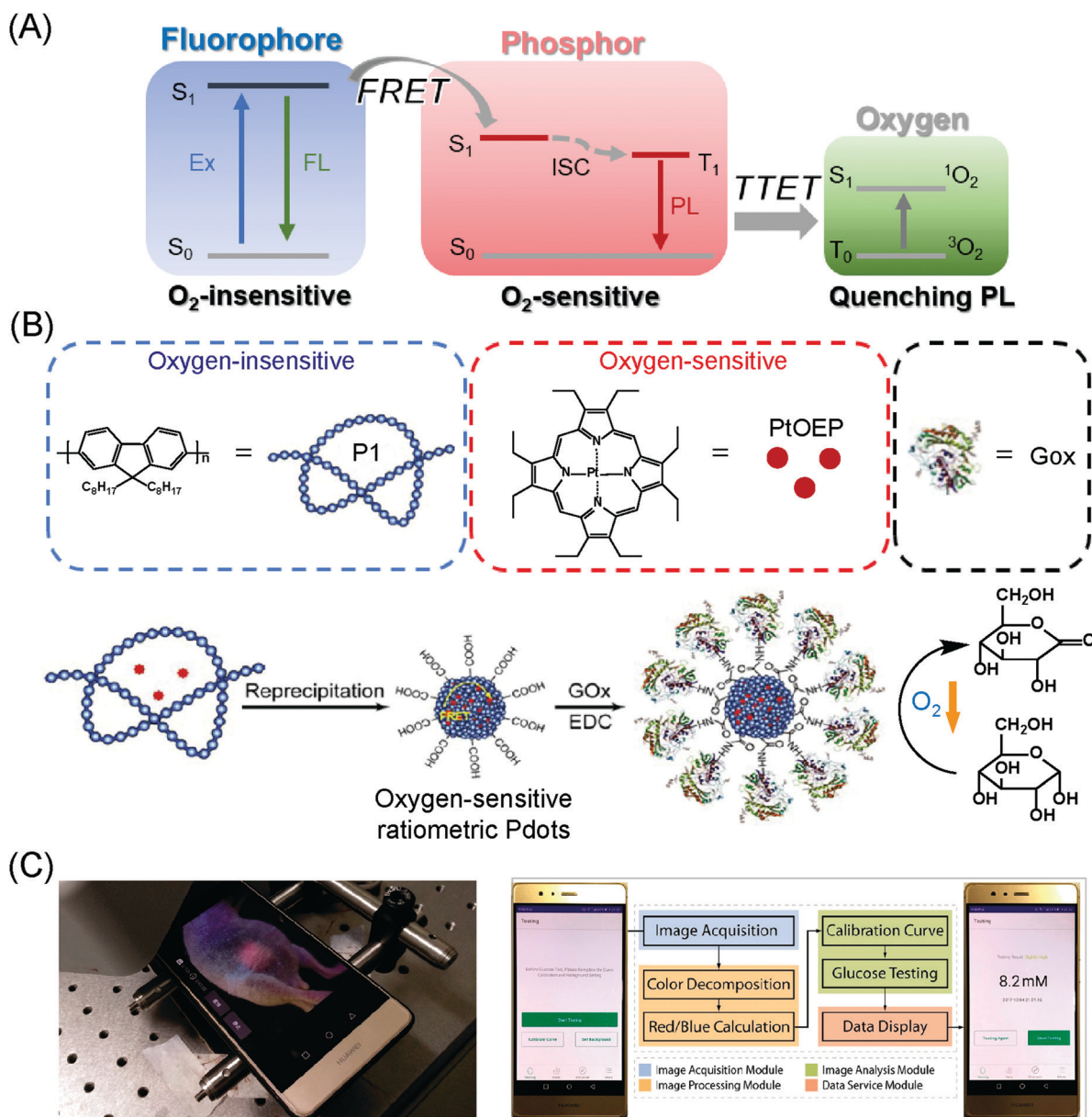
Fig. 12 (A) Mechanism of the fluorescent/phosphorescent ratiometric probes for oxygen sensing. (B) Chemical structures of luminophores used for the construction of oxygen-sensitive ratiometric Pdots and the schematic illustration of the design principle for constructing Pdot–GOx bioconjugates in glucose monitoring. Reproduced with permission from ref. 105. Copyright 2016 American Chemical Society. (C) Photograph of the site of interest in live mice using a smartphone camera and the developed APP is used to decompose and analyse glucose-related data. Reproduced with permission from ref. 106. Copyright 2018 American Chemical Society.

7322 | *J. Mater. Chem. B*, 2022, **10**, 7309–7327

This journal is © The Royal Society of Chemistry 2022

participated reaction. In such studies, the responsive group was preferably designed as the energy transfer acceptor and the chemical structure of the acceptors did not change either in the presence or absence of analytes. Therefore, according to this strategy, the energy transfer process in the designed probe was kept stable, resulting in a stable emission of the reference signal and analyte concentrations dependent on the response fluorescence signal of the probe. It is noteworthy that the ratiometric CP-based probes designed following this strategy were mostly reusable and could be used for quantitative detection, but their detection sensitivity absolutely depended on the properties of the response groups, and the sensitivity amplification effect of energy transfer process was inapplicable.

Oxygen is a vital component for living cells, as it is associated with many physiological and pathological processes.[95–99] Phosphorescent transition-metal complexes have been widely employed for the detection of the oxygen concentration by utilizing the highly efficient triplet–triplet energy transfer (TTET) from the triplet excited state of the metal complex to the triplet ground state of oxygen, which resulted in a phosphorescence decrease with the increased oxygen concentration (Fig. 12A).[100–103] On the basis of such properties of phosphorescent complexes, Wu *et al.* proposed a novel strategy for designing the oxygen-sensitive ratiometric nanoprobe by co-doping CPs (P1) and platinum(ɪɪ) octaethylporphyrin complexes (PtOEP).[104] With an excitation wavelength of 380 nm, the efficient intra-particle energy transfer from photon-capturing polymer P1 (the energy transfer donor) to the phosphorescent oxygen-sensitive PtOEP (the energy transfer accepter) resulted in dual emission bands at 440 nm and 650 nm, respectively. When suspending Pdots in aqueous solution, an intense red emission under flowing nitrogen was observed, while the air- and oxygen-saturated Pdot solutions presented weak phosphorescence emission. Notably, the intensity of the fluorescence signal from P1 was almost kept constant as a reference signal. In addition, the measurement of luminescence lifetimes under different oxygen concentrations could realize accurate and reliable quantitative oxygen sensing, which confirmed high feasibility of the ratiometric nanoprobe.

Inspired by the enzyme-catalyzed reactions accompanied by the consumption or generation of oxygen, Sun *et al.* put forward a strategy to monitor the concentration of glucose by using the ratiometric luminescent O_2 transducers.[105] Similar to the strategies mentioned above, the transducer comprised CPs doped with oxygen-sensitive phosphorescent PtOEP. As shown in Fig. 12B, the surface of the glucose transducer was functionalized with glucose oxidase (GOx). Without glucose, the dissolved oxygen concentration would remain unchanged and the solution would exhibit weak luminescence under the quenching of oxygen. In the presence of glucose, the Gox-catalysed oxide reaction of glucose consumed the oxygen rapidly, resulting in a decreased concentration of dissolved oxygen. Then, an enhanced phosphorescent emission of Pdots was observed. By monitoring the blue fluorescent signal and red phosphorescent emission of Pdots, the sensitive detection and real-time monitoring of glucose could be realized. Notably,

this strategy could be generalized for monitoring a series of oxygen-related physiological processes *in vivo*. Besides, an image-processing algorithm was developed and installed using a smartphone for the wireless dynamic monitoring of glucose *in vivo*, with the existence of the implanted transducer (Fig. 12C).[106] Moreover, by using hydrogels as the carriers of Pdots, such a transducer for the long-term monitoring of glucose *in vivo* was realized.[107]

Nonetheless, the above-mentioned strategies for constructing ratiometric oxygen-sensitive probes that we discussed in this section were based on the co-doped single-band emissive CPs and oxygen-sensitive phosphor, which might suffer from leakage and would lead to erroneous measurements and misleading conclusions. In contrast, covalently coupling the CPs and functional group into a single one molecule could avoid the escaping of crucial indicators. In 2012, Xiang *et al.* reported the practice of attaching platinum(ɪɪ) porphyrin complexes to the backbone of the CPs covalently which helped in realizing the construction of ratiometric luminescent oxygen-sensitive conjugated polymers.[108] However, in this work, the applicability of such a sensor in aqueous solutions and the biological environment has not been identified. To develop a water-soluble probe for oxygen sensing, Shi *et al.* introduced phosphorescent Ir(ɪɪɪ) complexes into the backbone of conjugated polymers and modified the side chains with hydrophilic polyether and quaternary ammonium group, which made ratiometric oxygen sensing in aqueous solutions possible (Fig. 13A).[109] With amphiphilic structures, the polymer could self-assemble to form oxygen-sensitive nanoprobes without no need for other modifications. Energy could be transferred efficiently from the backbone of the polymers to Ir(ɪɪɪ) complexes in this oxygen sensing platform. The emission spectrum was dominated by the phosphorescent emission from the Ir(ɪɪɪ) complex at 630 nm, in the nitrogen environment. However, the intensity of the red emission decreased remarkably with the increase in the oxygen concentration accompanied with luminescent colour being changed from red to blue under the excitation at 365 nm. Throughout, the blue fluorescence signal which could be attributed to the polymer backbones, existed as the reference signal with a little intensity change. Moreover, the adoption of photoluminescence lifetime imaging microscopy (PLIM) and time-gated luminescence imaging (TGLI) increased the possibility of the measurement and imaging in complexed media. After replacing Ir(ɪɪɪ) complexes with Pt(ɪɪ) porphyrin complexes, a ratiometric responsive oxygen sensor with a longer emission wavelength and a longer emission lifetime was obtained (Fig. 13B).[43] This probe was employed in imaging and monitoring of tumor hypoxia *in vivo*, evidencing the capability of this probe in small animals. A similar dual emissive oxygen sensor was developed by substituting some of the polyfluorene in P19 and P20 with BODIPY derivatives, and it displayed an extended excitation wavelength in the visible optical region and amplified singlet oxygen generation capacity and oxygen sensitivity. As shown in Fig. 13C, conjugated polymers and BODIPY derivatives served as the energy donor, which enhanced the light-harvesting capability of the
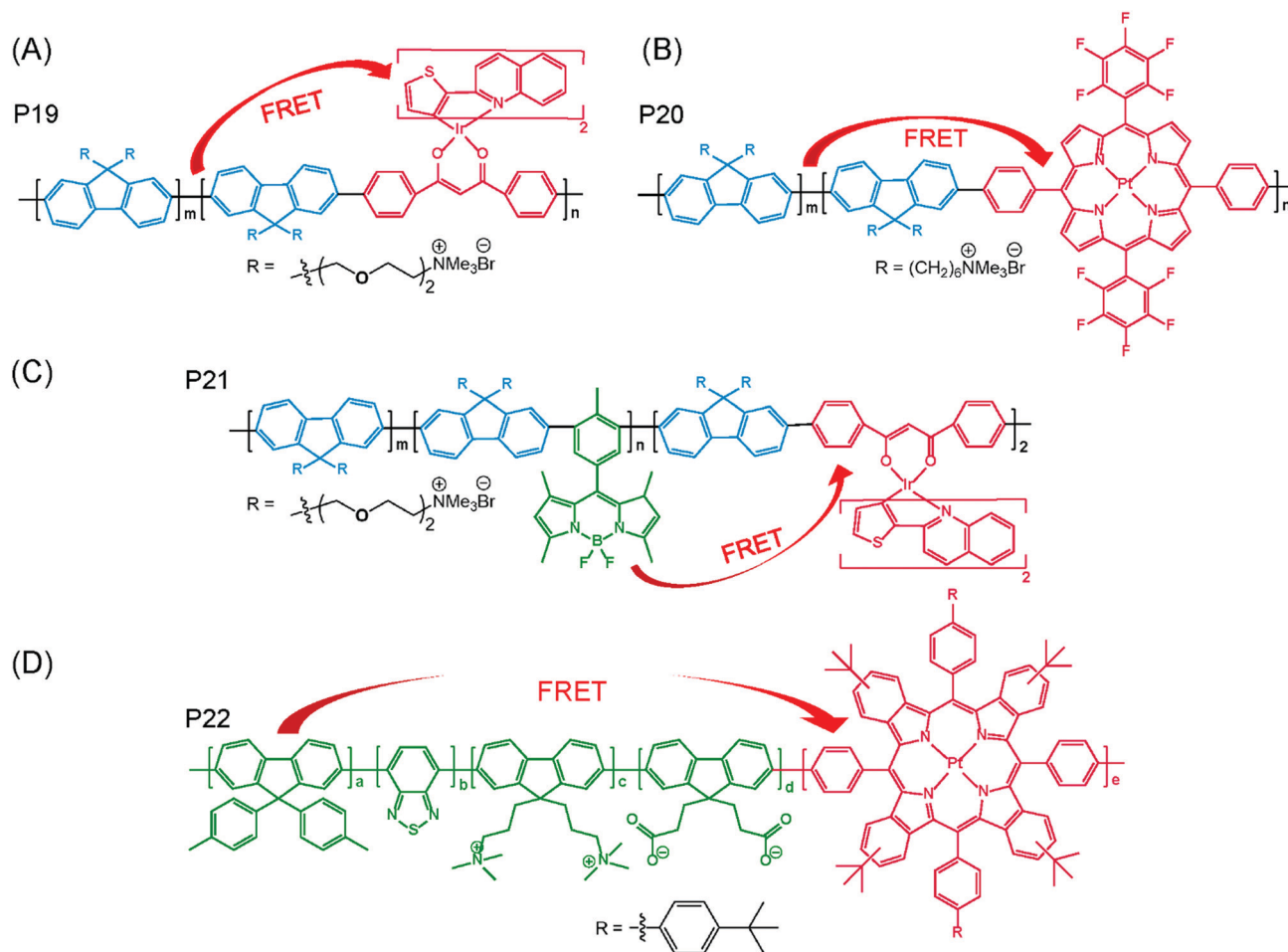
This journal is © The Royal Society of Chemistry 2022

J. Mater. Chem. B, 2022, **10**, 7309–7327 | **7323**

Fig. 13 Chemical structures of the ratiometric luminescent probes for oxygen detection that constructed by immobilize the oxygen-sensitive transition metal complexes into the backbone of conjugated polymers (A-P19, B-P20, C-P21 and D-P22).

Pdots. Ir(III) complexes served as the energy acceptor, which lead to high detection sensitivity and high generation yield of singlet oxygen. The superiority of such a concept for constructing ratiometric oxygen sensors was further confirmed by other studies (Fig. 13D).[110,111] In addition, to reduce the potential aggregation-induced quenching of traditional linear structures, hyper-branched conjugated polymers were employed for the construction of oxygen-sensitive probes with enhanced performance.[112,113] Besides, the design principles of oxygen-sensitive probes have been further employed in the ratiometric measurement and sensing of tyrosinase activity[114] and NADH.[115,116]

4. Conclusion and future perspective

In contrast to traditional single-wavelength emission intensity-dependent probes, CP-based ratiometric optical probes are proved to be capable of eliminating fluctuations and ambiguities caused by analyte-independent factors, providing insights for constructing ultra-bright and more reliable sensors in biomolecular sensing and bioimaging. Significant progress has been achieved in the construction of CP-based ratiometric

luminescent probes. In this review, we have summarized the various design principles of luminescent conjugated polymers developed for the ratiometric measurement of biomolecules. Additionally, major challenges and research advances of these CP-based luminescent probes in accurate biodetection were analyzed and discussed. The signal amplification effect of conjugated polymers can bring about obvious sensitivity improvement of these sensing probes in biodetection applications. As reported in many studies, the introduction of CPs has also been proved to be a highly effective strategy in biomedical detection because of their excellent properties.

Although CP-based ratiometric sensing and imaging strategies have been demonstrated *in vitro* and *in vivo*, there are still several challenges that should not be neglected. The following issues deserve more attention in future CP-based ratiometric luminescent probe explorations.

First, the most commonly reported CP-based ratiometric probes work by monitoring different emission signals in two or more channels, which could easily be distributed in the visible region. Considering different absorption and scattering capacities of the tissues to photons under different wave-lengths, such ratiometric probes may not be suitable for

7324 | *J. Mater. Chem. B*, 2022, **10**, 7309–7327

This journal is © The Royal Society of Chemistry 2022

accurate detection *in vivo*. Future studies on conjugated polymer-based probes in accurate detection *in vivo* should focus more on developing conjugated polymer materials with NIR absorption and emission properties since these materials exhibit better tissue penetration and higher imaging resolution.

Second, CP-based ratiometric detection and sensing strategies mainly focus on the energy transfer between CPs and organic dyes. Only a few studies have investigated the energy transfer between CPs and their cohorts or between CPs and other types of energy acceptors in order to improve the performance of luminescent probes in biosensing and bioimaging. To this end, more attempts need to be made for determining the optimal combination of CP-based ratiometric sensing platforms.

Finally, many aspects such as theoretical calculations, molecular modelling, surface chemistry, and pharmacokinetics are still worth investigating and we should provide constructive suggestions for the subsequent optimization of the structure and properties. Undoubtedly, reproducibility of the batch production of CPs is also an urgent goal to be achieved.

In brief, progress towards the development of ratiometric detection and sensing based on CPs in recent years is remarkable, and further exploration may promote the liquid biopsy and point-of-care testing (POCT). Meanwhile, the structure–function relationship and synergistic therapy still need to be designed and explored in-depth and in detail, so as to promote precision medicine.

Conflicts of interest

There are no conflicts to declare.

Acknowledgements

Notes and references

1 M. Labib, E. H. Sargent and S. O. Kelley, *Chem. Rev.*, 2016, **116**, 9001–9090.

2 I. Pereiro, J. F. Cors, S. Pane, B. J. Nelson and G. V. Kaigala, *Chem. Soc. Rev.*, 2019, **48**, 1236–1254.

3 F. Li, J. Li, B. Dong, F. Wang, C. Fan and X. Zuo, *Chem. Soc. Rev.*, 2021, **50**, 5650–5667.

4 S. H. Yun and S. J. J. Kwok, *Nat. Biomed. Eng.*, 2017, **1**, 0008.

5 S. Waite, A. Grigorian, R. G. Alexander, S. L. Macknik, M. Carrasco, D. J. Heeger and S. Martinez-Conde, *Front. Hum. Neurosci.*, 2019, **13**, 213.

6 C. Lu, L. Han, J. Wang, J. Wan, G. Song and J. Rao, *Chem. Soc. Rev.*, 2021, **50**, 8102–8146.

7 M. T. Ghoneim, A. Nguyen, N. Dereje, J. Huang, G. C. Moore, P. J. Murzynowski and C. Dagdeviren, *Chem. Rev.*, 2019, **119**, 5248–5297.

8 J. A. Thomas, *Chem. Soc. Rev.*, 2015, **44**, 4494–4500.

9 J. S. D. Mieog, F. B. Achterberg, A. Zlitni, M. Hutteman, J. Burggraaf, R. J. Swijnenburg, S. Gioux and A. L. Vahrmeijer, *Nat. Rev. Clin. Oncol.*, 2022, **19**, 9–22.

10 Y. Zhang, G. Zhang, Z. Zeng and K. Pu, *Chem. Soc. Rev.*, 2022, **51**, 566–593.

11 H. A. Clark, R. Kopelman, R. Tjalkens and M. A. Philbert, *Anal. Chem.*, 1999, **71**, 4837–4843.

12 L. Yuan, W. Lin, K. Zheng and S. Zhu, *Acc. Chem. Res.*, 2013, **46**, 1462–1473.

13 X. Huang, J. Song, B. C. Yung, X. Huang, Y. Xiong and X. Chen, *Chem. Soc. Rev.*, 2018, **47**, 2873–2920.

14 R. Gui, H. Jin, X. Bu, Y. Fu, Z. Wang and Q. Liu, *Coord. Chem. Rev.*, 2019, **383**, 82–103.

15 L. Wu, C. Huang, B. P. Emery, A. C. Sedgwick, S. D. Bull, X. P. He, H. Tian, J. Yoon, J. L. Sessler and T. D. James, *Chem. Soc. Rev.*, 2020, **49**, 5110–5139.

16 X. Jiang, J. Chen, A. Bajic, C. Zhang, X. Song, S. L. Carroll, Z. L. Cai, M. Tang, M. Xue, N. Cheng, C. P. Schaaf, F. Li, K. R. MacKenzie, A. C. M. Ferreon, F. Xia, M. C. Wang, M. Maletic-Savatic and J. Wang, *Nat. Commun.*, 2017, **8**, 16087.

17 Z. Liu, X. Zhou, Y. Miao, Y. Hu, N. Kwon, X. Wu and J. Yoon, *Angew. Chem., Int. Ed.*, 2017, **56**, 5812–5816.

18 K. Umezawa, M. Yoshida, M. Kamiya, T. Yamasoba and Y. Urano, *Nat. Chem.*, 2017, **9**, 279–286.

19 K. Umezawa, M. Kamiya and Y. Urano, *Angew. Chem., Int. Ed.*, 2018, **57**, 9346–9350.

20 S. Cheng, B. Shen, W. Yuan, X. Zhou, Q. Liu, M. Kong, Y. Shi, P. Yang, W. Feng and F. Li, *ACS Cent. Sci.*, 2019, **5**, 299–307.

21 S. Zhang, H. Chen, L. Wang, X. Qin, B. P. Jiang, S. C. Ji, X. C. Shen and H. Liang, *Angew. Chem., Int. Ed.*, 2022, **61**, e202107076.

22 O. S. Wolfbeis, *Chem. Soc. Rev.*, 2015, **44**, 4743–4768.

23 W. R. Algar, M. Massey, K. Rees, R. Higgins, K. D. Krause, G. H. Darwish, W. J. Peveler, Z. Xiao, H. Y. Tsai, R. Gupta, K. Lix, M. V. Tran and H. Kim, *Chem. Rev.*, 2021, **121**, 9243–9358.

24 H. Yuan, B. Wang, F. Lv, L. Liu and S. Wang, *Adv. Mater.*, 2014, **26**, 6978–6982.

25 F. Lv, T. Qiu, L. Liu, J. Ying and S. Wang, *Small*, 2016, **12**, 696–705.

26 J. Wei, Y. Liu, J. Yu, L. Chen, M. Luo, L. Yang, P. Li, S. Li and X. H. Zhang, *Small*, 2021, **17**, e2103127.

27 C. Wu and D. T. Chiu, *Angew. Chem., Int. Ed.*, 2013, **52**, 3086–3109.

28 H. S. Peng and D. T. Chiu, *Chem. Soc. Rev.*, 2015, **44**, 4699–4722.

This journal is © The Royal Society of Chemistry 2022

J. Mater. Chem. B, 2022, **10**, 7309–7327 | **7325**

29 Y. Wang, L. Feng and S. Wang, *Adv. Funct. Mater.*, 2019, **29**, 1806818.

30 L. Feng, L. Liu, F. Lv, G. C. Bazan and S. Wang, *Adv. Mater.*, 2014, **26**, 3926–3930.

31 Z. Chen, X. Meng, L. Zou, M. Zhao, S. Liu, P. Tao, J. Jiang and Q. Zhao, *ACS Appl. Mater. Interfaces*, 2020, **12**, 12383–12394.

32 Z. Chen, X. Meng, M. Xie, Y. Shi, L. Zou, S. Guo, J. Jiang, S. Liu and Q. Zhao, *J. Mater. Chem. C*, 2020, **8**, 2265–2271.

33 F. Feng, L. Liu, Q. Yang and S. Wang, *Macromol. Rapid Commun.*, 2010, **31**, 1405–1421.

34 X. Feng, L. Liu, S. Wang and D. Zhu, *Chem. Soc. Rev.*, 2010, **39**, 2411–2419.

35 Z. Tian, J. Yu, C. Wu, C. Szymanski and J. McNeill, *Nanoscale*, 2010, **2**, 1999–2011.

36 C. Zhu, L. Liu, Q. Yang, F. Lv and S. Wang, *Chem. Rev.*, 2012, **112**, 4687–4735.

37 L. Feng, C. Zhu, H. Yuan, L. Liu, F. Lv and S. Wang, *Chem. Soc. Rev.*, 2013, **42**, 6620–6633.

38 T. Repenko, A. Rix, S. Ludwanowski, D. Go, F. Kiessling, W. Lederle and A. J. C. Kuehne, *Nat. Commun.*, 2017, **8**, 470.

39 H. Shi, H. Sun, H. Yang, S. Liu, G. Jenkins, W. Feng, F. Li, Q. Zhao, B. Liu and W. Huang, *Adv. Funct. Mater.*, 2013, **23**, 3268–3276.

40 C. Z. Wang, J. L. Chen, Y. Tang, Y. Zang, G. R. Chen, T. D. James, J. Li, C. Wu and X. P. He, *ACS Appl. Mater. Interfaces*, 2017, **9**, 3272–3276.

41 L. Chen, L. Wu, J. Yu, C. T. Kuo, T. Jian, I. C. Wu, Y. Rong and D. T. Chiu, *Chem. Sci.*, 2017, **8**, 7236–7245.

42 L. Wu, I. C. Wu, C. C. DuFort, M. A. Carlson, X. Wu, L. Chen, C. T. Kuo, Y. Qin, J. Yu, S. R. Hingorani and D. T. Chiu, *J. Am. Chem. Soc.*, 2017, **139**, 6911–6918.

43 Q. Zhao, X. Zhou, T. Cao, K. Y. Zhang, L. Yang, S. Liu, H. Liang, H. Yang, F. Li and W. Huang, *Chem. Sci.*, 2015, **6**, 1825–1831.

44 Z. Liu, W. He and Z. Guo, *Chem. Soc. Rev.*, 2013, **42**, 1568–1600.

45 A. S. Klymchenko, *Acc. Chem. Res.*, 2017, **50**, 366–375.

46 S. Wu, H. Min, W. Shi and P. Cheng, *Adv. Mater.*, 2020, **32**, e1805871.

47 J. Song, J. Zhang, F. Lv, Y. Cheng, B. Wang, L. Feng, L. Liu and S. Wang, *Angew. Chem., Int. Ed.*, 2013, **52**, 13020–13023.

48 J. Song, Q. Yang, F. Lv, L. Liu and S. Wang, *ACS Appl. Mater. Interfaces*, 2012, **4**, 2885–2890.

49 J. Zhang, B. Xing, J. Song, F. Zhang, C. Nie, L. Jiao, L. Liu, F. Lv and S. Wang, *Anal. Chem.*, 2014, **86**, 346–350.

50 X. Feng, X. Duan, L. Liu, F. Feng, S. Wang, Y. Li and D. Zhu, *Angew. Chem., Int. Ed.*, 2009, **48**, 5316–5321.

51 L. An, Y. Tang, S. Wang, Y. Li and D. Zhu, *Macromol. Rapid Commun.*, 2006, **27**, 993–997.

52 X. Duan, L. Liu, X. Feng and S. Wang, *Adv. Mater.*, 2010, **22**, 1602–1606.

53 X. Liu, L. Ouyang, Y. Huang, X. Feng, Q. Fan and W. Huang, *Polym. Chem.*, 2012, **3**, 703–709.

54 X. Liu, L. Ouyang, X. Cai, Y. Huang, X. Feng, Q. Fan and W. Huang, *Biosens. Bioelectron.*, 2013, **41**, 218–224.

55 L. An, L. Liu, S. Wang and G. C. Bazan, *Angew. Chem., Int. Ed.*, 2009, **48**, 4372–4375.

56 F. He, M. Yu and S. Wang, *Sci. Bull.*, 2009, **54**, 1340–1344.

57 F. Feng, H. Wang, L. Han and S. Wang, *J. Am. Chem. Soc.*, 2008, **130**, 11338–11343.

58 Q. Yang, T. Qiu, W. Wu, C. Zhu, L. Liu, J. Ying and S. Wang, *ACS Appl. Mater. Interfaces*, 2011, **3**, 4539–4545.

59 L. Ma, Y. Huang, H. Zhang, W. Ning, R. Qi, H. Yuan, F. Lv, L. Liu, C. Yu and S. Wang, *ACS Appl. Mater. Interfaces*, 2021, **13**, 9291–9299.

60 I. Capila and R. J. Linhardt, *Angew. Chem., Int. Ed.*, 2002, **41**, 390–412.

61 K.-Y. Pu and B. Liu, *Adv. Funct. Mater.*, 2009, **19**, 277–284.

62 K.-Y. Pu, L. Cai and B. Liu, *Macromolecules*, 2009, **42**, 5933–5940.

63 K. Pu, R. Zhan, J. Liang and B. Liu, *Sci. China: Chem.*, 2011, **54**, 567–574.

64 R. T. K. Kwok, J. Geng, J. W. Y. Lam, E. Zhao, G. Wang, R. Zhan, B. Liu and B. Z. Tang, *J. Mater. Chem. B*, 2014, **2**, 4134–4141.

65 K.-Y. Pu and B. Liu, *Macromolecules*, 2008, **41**, 6636–6640.

66 J. Shi, K.-Y. Pu, R. Zhan and B. Liu, *Macromol. Chem. Phys.*, 2009, **210**, 1195–1200.

67 H. Shi, X. Chen, S. Liu, H. Xu, Z. An, L. Ouyang, Z. Tu, Q. Zhao, Q. Fan, L. Wang and W. Huang, *ACS Appl. Mater. Interfaces*, 2013, **5**, 4562–4568.

68 Q. Cui, Y. Yang, C. Yao, R. Liu and L. Li, *ACS Appl. Mater. Interfaces*, 2016, **8**, 35578–35586.

69 Q. Zhao, Z. Zhang and Y. Tang, *Chem. Commun.*, 2017, **53**, 9414–9417.

70 S. Zhu, X. Wang, Y. Yang, H. Bai, Q. Cui, H. Sun, L. Li and S. Wang, *Chem. Mater.*, 2018, **30**, 3244–3253.

71 N. Zehra, D. Dutta, A. H. Malik, S. S. Ghosh and P. K. Iyer, *ACS Appl. Mater. Interfaces*, 2018, **10**, 27603–27611.

72 S. Y. Kuo, H. H. Li, P. J. Wu, C. P. Chen, Y. C. Huang and Y. H. Chan, *Anal. Chem.*, 2015, **87**, 4765–4771.

73 C. Z. Wang, H. H. Han, X. Y. Tang, D. M. Zhou, C. Wu, G. R. Chen, X. P. He and H. Tian, *ACS Appl. Mater. Interfaces*, 2017, **9**, 25164–25170.

74 D. E. Clapham, *Cell*, 2007, **131**, 1047–1058.

75 H. Kuboniwa, N. Tjandra, S. Grzesiek, H. Ren, C. B. Klee and A. Bax, *Nat. Struct. Mol. Biol.*, 1995, **2**, 768–776.

76 H. Yuan, J. Qi, C. Xing, H. An, R. Niu, Y. Zhan, Y. Fan, W. Yan, R. Li, B. Wang and S. Wang, *Adv. Funct. Mater.*, 2015, **25**, 4412–4418.

77 A. R. Lippert, G. C. Van de Bittner and C. J. Chang, *Acc. Chem. Res.*, 2011, **44**, 793–804.

78 Y. Wang, S. Li, L. Feng, C. Nie, L. Liu, F. Lv and S. Wang, *ACS Appl. Mater. Interfaces*, 2015, **7**, 24110–24118.

79 M. Shamsipur, A. Barati and Z. Nematifar, *J. Photochem. Photobiol., C*, 2019, **39**, 76–141.

80 A. Steinegger, O. S. Wolfbeis and S. M. Borisov, *Chem. Rev.*, 2020, **120**, 12357–12489.

81 Q. Bai, C. Yang, M. Yang, Z. Pei, X. Zhou, J. Liu, H. Ji, G. Li, M. Wu, Y. Qin, Q. Wang and L. Wu, *Anal. Chem.*, 2022, **94**, 2901–2911.

7326 | *J. Mater. Chem. B*, 2022, **10**, 7309–7327

This journal is © The Royal Society of Chemistry 2022

82 Y. H. Chan, C. Wu, F. Ye, Y. Jin, P. B. Smith and D. T. Chiu, *Anal. Chem.*, 2011, **83**, 1448–1455.

83 B. Bao, P. Su, Z. Yang, X. Zhai, J. Zhang, Y. Xu, Y. Liu, B. Gu and L. Wang, *Adv. Healthcare Mater.*, 2019, **8**, e1900255.

84 W. Xu, S. Lu, M. Xu, Y. Jiang, Y. Wang and X. Chen, *J. Mater. Chem. B*, 2016, **4**, 292–298.

85 Q. Zhang, J. Sun, R. Zhang, X. Chen, N. Chen and F. Gao, *Chem. Commun.*, 2020, **56**, 8647–8650.

86 K. Apel and H. Hirt, *Annu. Rev. Plant Biol.*, 2004, **55**, 373–399.

87 R. Medzhitov, *Nature*, 2008, **454**, 428–435.

88 J. M. Mates, J. A. Segura, F. J. Alonso and J. Marquez, *Arch. Toxicol.*, 2012, **86**, 1649–1665.

89 A. Weidinger and A. V. Kozlov, *Biomolecules*, 2015, **5**, 472–484.

90 H. Sies and D. P. Jones, *Nat. Rev. Mol. Cell Biol.*, 2020, **21**, 363–383.

91 K. Pu, A. J. Shuhendler and J. Rao, *Angew. Chem., Int. Ed.*, 2013, **52**, 10325–10329.

92 D. Oushiki, H. Kojima, T. Terai, M. Arita, K. Hanaoka, Y. Urano and T. Nagano, *J. Am. Chem. Soc.*, 2010, **132**, 2795–2801.

93 W. Hou, Y. Yuan, Z. Sun, S. Guo, H. Dong and C. Wu, *Anal. Chem.*, 2018, **90**, 14629–14634.

94 Q. Zhang, X. Hu, X. Dai, P. Ling, J. Sun, H. Chen and F. Gao, *ACS Nano*, 2021, **15**, 13633–13645.

95 T. Acker and H. Acker, *J. Exp. Biol.*, 2004, **207**, 3171–3188.

96 M. Höckel, K. Schlenger, S. Höckel, B. Aral, U. Schäffer and P. Vaupel, *Int. J. Cancer*, 1998, **79**, 365–369.

97 P. Carmeliet, Y. Dor, J.-M. Herbert, D. Fukumura, K. Brusselmans, M. Dewerchin, M. Neeman, F. Bono, R. Abramovitch, P. Maxwell, C. J. Koch, P. Ratcliffe, L. Moons, R. K. Jain, D. Collen and E. Keshet, *Nature*, 1998, **394**, 485–490.

98 J. H. Distler, R. H. Wenger, M. Gassmann, M. Kurowska, A. Hirth, S. Gay and O. Distler, *Arthritis Rheum.*, 2004, **50**, 10–23.

99 G. L. Semenza, *Science*, 2007, **318**, 62–64.

100 W. L. Rumsey, J. M. Vanderkooi and D. F. Wilson, *Science*, 1988, **241**, 1649–1651.

101 H. Xu, J. W. Aylott, R. Kopelman, T. J. Miller and M. A. Philbert, *Anal. Chem.*, 2001, **73**, 4124–4133.

102 Y.-E. L. Koo, Y. Cao, R. Kopelman, S. M. Koo, M. Brasuel and M. A. Philbert, *Anal. Chem.*, 2004, **76**, 2498–2505.

103 E. Ikeda, *Pathol. Int.*, 2005, **55**, 603–610.

104 C. Wu, B. Bull, K. Christensen and J. McNeill, *Angew. Chem., Int. Ed.*, 2009, **48**, 2741–2745.

105 K. Sun, Y. Tang, Q. Li, S. Yin, W. Qin, J. Yu, D. T. Chiu, Y. Liu, Z. Yuan, X. Zhang and C. Wu, *ACS Nano*, 2016, **10**, 6769–6781.

106 K. Sun, Y. Yang, H. Zhou, S. Yin, W. Qin, J. Yu, D. T. Chiu, Z. Yuan, X. Zhang and C. Wu, *ACS Nano*, 2018, **12**, 5176–5184.

107 J. Liu, X. Fang, Z. Zhang, Z. Liu, J. Liu, K. Sun, Z. Yuan, J. Yu, D. T. Chiu and C. Wu, *Anal. Chem.*, 2022, **94**, 2901–2911.

108 H. Xiang, L. Zhou, Y. Feng, J. Cheng, D. Wu and X. Zhou, *Inorg. Chem.*, 2012, **51**, 5208–5212.

109 H. Shi, X. Ma, Q. Zhao, B. Liu, Q. Qu, Z. An, Y. Zhao and W. Huang, *Adv. Funct. Mater.*, 2014, **24**, 4823–4830.

110 R. I. Dmitriev, S. M. Borisov, H. Düssmann, S. Sun, B. J. Müller, J. Prehn, V. P. Baklaushev, I. Klimant and D. B. Papkovsky, *ACS Nano*, 2015, **9**, 5275–5288.

111 G. Li, T. Huang, M. Xie, X. Zhang, Q. Yu, S. Liu, T. Yang and Q. Zhao, *J. Organomet. Chem.*, 2019, **879**, 144–149.

112 X. Zhou, H. Liang, P. Jiang, K. Y. Zhang, S. Liu, T. Yang, Q. Zhao, L. Yang, W. Lv, Q. Yu and W. Huang, *Adv. Sci.*, 2016, **3**, 1500155.

113 Z. Feng, P. Tao, L. Zou, P. Gao, Y. Liu, X. Liu, H. Wang, S. Liu, Q. Dong, J. Li, B. Xu, W. Huang, W. Y. Wong and Q. Zhao, *ACS Appl. Mater. Interfaces*, 2017, **9**, 28319–28330.

114 J. Sun, H. Mei, S. Wang and F. Gao, *Anal. Chem.*, 2016, **88**, 7372–7377.

115 H. Chen, J. Yu, X. Men, J. Zhang, Z. Ding, Y. Jiang, C. Wu and D. T. Chiu, *Angew. Chem., Int. Ed.*, 2021, **60**, 12007–12012.

116 H. Chen, J. Yu, J. Zhang, K. Sun, Z. Ding, Y. Jiang, Q. Hu, C. Wu and D. T. Chiu, *Angew. Chem., Int. Ed.*, 2021, **60**, 19331–19336.

This journal is © The Royal Society of Chemistry 2022

J. Mater. Chem. B, 2022, **10**, 7309–7327 | **7327**